Stable charging of a Rydberg quantum battery in an open system

Y. Yao and X. Q. Shao [*]

Center for Quantum Sciences and School of Physics, Northeast Normal University, Changchun 130024, China
and Center for Advanced Optoelectronic Functional Materials Research, and Key Laboratory for UV Light-Emitting Materials and
Technology of Ministry of Education, Northeast Normal University, Changchun 130024, China

The charging of an open quantum battery is investigated where the charger and the quantum battery interact with a common environment. At zero temperature, the stored energy of the battery is optimal as the charger and the quantum battery share the same coupling strength ($g_C = g_B$). By contrast, in the presence of the quantum jump-based feedback control, the energy stored in the battery can be greatly enhanced for different couplings ($g_C > g_B$). Considering the feasibility of the experiment, a model of Rydberg quantum battery is proposed with cascade-type atoms interacting with a dissipative optical cavity. The effective coupling strength between the charger (quantum battery) and the cavity field is hence adjustable and one can make the battery close to perfect excitation. The adverse factors of charging quantum batteries such as time delay for feedback, finite temperature, and spontaneous emission of Rydberg atoms are also discussed, and the result shows that the quantum battery is still able to retain a satisfactory energy storage effect.

I. INTRODUCTION

Conventional batteries are devices that convert chemical energy into electrical energy, with positive and negative electrodes. With the progress of science and technology, batteries generally refer to small devices that can generate electric energy, such as solar cells [1]. In recent years, the concept of quantum batteries (QBs) was proposed by Alicki and Fannes [2]. They defined a QB as a small quantum mechanical system that is used to store or extract energy. As we all know, quantum entanglement [3,4], quantum coherence [5], and quantum discord [6,7] have been viewed as physical resources to apply in many high-tech and basic research fields, such as quantum teleportation [8,9], quantum image [10], quantum radar [11], quantum computing [12–14], etc. This greatly inspires researchers' interest in QB, as they hope to get a kind of battery with better performance than a traditional battery by using the characteristic of quantum correlation.

Initially, QBs were modeled as a series of two-level systems to explore properties in a closed system, such as stored energy, charging power, and ergotropy [15–30]. There are two forms of charging: One is parallel charging [18,20], in which each QB is charged by corresponding charger and independent of each other; the other is collective charging [2,15,16,19,21], where all the QBs are charged by the same charger. Some scientists have come to the conclusion that collective charging has more performance advantages than individual charging. The above schemes correspond to the unitary evolution of the QB driven by time-dependent Hamiltonian. Due to the coherent coupling between the QB and the charger, the stored energy of the QB is oscillating, which is strictly dependent

on the interaction time between the charger and the QB [20]. Once the optimal time is missed, the energy stored by the QB will be lower than the optimal energy value. To overcome this problem, some works have proposed adiabatic battery charging schemes to ensure a stable value for the QB charging instead of oscillating over time [31–34].

Open QBs are attended for solving the problem of QBs charging in open systems [35–50]. The inevitable interaction between the quantum system and the surrounding environment is not always detrimental to quantum properties [51,52]. Thus, some researchers suggest that the environment should be regarded as a resource to assist QB charging. For instance, Ito and Watanabe utilized a quantum heat engine to charge the QBs and obtained a QBs with high power and high capacity [37]. And an experiment based on Dicke QBs [39] showed that by fine-tuning the decoherence process, the QBs can be charged quickly, and the corresponding discharge speed is much slower, which is conducive to the energy retention of the QBs. Therefore, noise environment is very important for the realization and application of QBs.

Recently, Quach and Munro [53] proposed a scheme of stable charging under a dissipative environment by using dark states. They modeled both the charger and the QB as a spin ensemble with the spin numbers of N_C and N_B, respectively. Then the charger and QB are coupled to a common reservoir with the same coupling strength, and there is no direct interaction between each other. When both the charger and the QB consist of one spin, the QB cannot be charged effectively. To improve the stored energy of the QB, it is necessary to increase the number of spins in the charger so that N_C is much greater than 1, which greatly wastes resources. Subsequently, Mitchison and Goold [54] proposed a QB scheme based on continuous weak measurements and feedback control. They assumed that the QB was an isolated system, and the external

[*]shaoxq644@nenu.edu.cn

environment deposited energy into the QB via the charger. In addition, the charger was a driven-dissipative two-level system that was subjected to a homodyne measurement, then the controller used the measurement record to adjust the laser intensity, resulting in stable and effective QB charging. However, in experiments, it was difficult to completely isolate the QB from the environment.

We know that the environment will decay the system to the ground state, which is not conducive to the charging of QB. To solve this problem, we introduce quantum jump-based feedback control into QB charging protocol. When the detector measures the decay signal of the system induced by atomic collective decay, it triggers the feedback control of the charger, and then actively controls the quantum system in a desired form to compensate for the impact of environmental on QB. This kind of quantum feedback control [55] have been widely used in quantum error correction [56,57], decoherence control [58,59], atomic cooling [60,61], entangled state preparation [62–64], and quantum optical experiments.

In our proposal, we consider both the charger and the QB interact with a common environment, which provides a channel for energy transfer from the charger to the QB. In Sec. II, we construct a theoretical model and investigate the effects of feedback control and coupling strength on storage and extraction of the QB energy. It is proved that when the coupling strengths of charger and QB to the environment are different, the stored energy of QB is increased greatly, only applying feedback control to the charger. In addition, we also discuss the energy cost of feedback. In Sec. III, we further put forward a corresponding physical model in which the charger and QB correspond to a cascaded Rydberg atom, respectively, and simultaneously reside in a dissipative optical cavity. When the detector D detects the photons leaking from the cavity field, the feedback control of the charger is triggered. Based on this physical model, discuss the effect of a small time delays, the effect of spontaneous emission, the effect of finite temperature and the scalability of QB for our scheme. In Sec. IV, we give a brief conclusion.

II. THEORETICAL MODEL

A. The master equation of the system

Typically, a charging scheme consists of a QB, an external energy source, or a charger. When the charger is coupled (decoupled) with the QB, the charging process is on (off). In this work, we regard the charger and the QB as two-level systems, respectively, each has an excited state $|e\rangle$ and a ground state $|g\rangle$. In addition, the charger and the QB are injected into a common reservoir; there is no direct interaction between the QB and the charger. Initially, the charger is in the excited state and the QB is in the ground state. We suppose that the charger and the QB have the same transition frequency, i.e., $\omega_C = \omega_B = \omega_0$, the total Hamiltonian of the system is $H = H_0 + H_I$, where ($\hbar = 1$)

$$H_0 = \omega_0 \sigma_C^+ \sigma_C^- + \omega_0 \sigma_B^+ \sigma_B^- + \sum_k \omega_k a_k^\dagger a_k, \quad (1)$$

$$H_I = \sum_k g_{Ck}(a_k^\dagger \sigma_C^- + a_k \sigma_C^+) + \sum_k g_{Bk}(a_k^\dagger \sigma_B^- + a_k \sigma_B^+), \quad (2)$$

where σ_i^+ and σ_i^- $(i = C, B)$ are the raising and lowering operators, respectively; ω_k, $a_k^\dagger$, and a_k are the frequency, creation, and annihilation operators, respectively, of the kth mode of the reservoir; and g_{ik} $(i = C, B)$ is the coupling constant between kth mode in the reservoir and the charger (QB). In the interaction picture, the Hamiltonian can be written as

$$H_{\text{int}} = \sum_k g_{Ck}[a_k^\dagger \sigma_C^- e^{-i(\omega_0 - \omega_k)t} + a_k \sigma_C^+ e^{i(\omega_0 - \omega_k)t}]$$
$$+ \sum_k g_{Bk}[a_k^\dagger \sigma_B^- e^{-i(\omega_0 - \omega_k)t} + a_k \sigma_B^+ e^{i(\omega_0 - \omega_k)t}]. \quad (3)$$

In the following, we consider a low temperature mechanism $(T = 0)$ into our scheme to guarantee that the energy of the reservoir is lower than ω_0. Therefore, the probability of photons absorbed from the reservoir can be ignored. With the Born-Markov approximation, the Lindblad master equation during charging process is

$$\dot{\rho} = \frac{\Gamma_C}{2}(2\sigma_C^- \rho \sigma_C^+ - \sigma_C^+ \sigma_C^- \rho - \rho \sigma_C^+ \sigma_C^-)$$
$$+ \frac{\Gamma_B}{2}(2\sigma_B^- \rho \sigma_B^+ - \sigma_B^+ \sigma_B^- \rho - \rho \sigma_B^+ \sigma_B^-)$$
$$+ \frac{\Gamma_1}{2}(2\sigma_C^- \rho \sigma_B^+ - \sigma_C^+ \sigma_B^- \rho - \rho \sigma_C^+ \sigma_B^-)$$
$$+ \frac{\Gamma_2}{2}(2\sigma_B^- \rho \sigma_C^+ - \sigma_B^+ \sigma_C^- \rho - \rho \sigma_B^+ \sigma_C^-), \quad (4)$$

where $\Gamma_C/2 \to \int_0^t dt' \sum_k g_{Ck}^2 e^{\pm(\omega_0 - \omega_k)(t-t')}$, $\Gamma_B/2 \to \int_0^t dt' \sum_k g_{Bk}^2 e^{\pm(\omega_0 - \omega_k)(t-t')}$ represent the pure spontaneous emission rates of charger and QB, and $\Gamma_1/2 = \Gamma_2/2 \to \int_0^t dt' \sum_k g_{Ck}g_{Bk}e^{\pm(\omega_0 - \omega_k)(t-t')}$ correspond to the cooperative spontaneous emission rates [65]. It should be noted that the last two items which will produce global entanglement between the charger and the QB without direct interaction.

B. Steady state and related energy of the system

For convenience, we now introduce $g_k = (g_{Ck}^2 + g_{Bk}^2)^{1/2}$. Therefore, $g_{Ck} = g_k g_{Ck}/(g_{Ck}^2 + g_{Bk}^2)^{1/2} = g_k \cos\theta$ and $g_{Bk} = g_k g_{Bk}/(g_{Ck}^2 + g_{Bk}^2)^{1/2} = g_k \sin\theta$, and $\theta = \arctan[g_{Bk}/g_{Ck}] \in (0, \pi/2)$. Subsequently, the above corresponding spontaneous emission rates can be rewritten as $\Gamma_C = \Gamma \cos\theta^2$, $\Gamma_B = \Gamma \sin\theta^2$, and $\Gamma_1 = \Gamma_2 = \Gamma \sin\theta \cos\theta$, respectively, and $\Gamma \to \int_0^t dt' \sum_k g_k^2 e^{\pm(\omega_0 - \omega_k)(t-t')}$. Then the above Lindblad master equation is reduced to

$$\dot{\rho} = \Gamma \mathcal{L}[J^-]\rho, \quad (5)$$

where $\mathcal{L}[o] \equiv o\rho o^\dagger - (o^\dagger o\rho + \rho o^\dagger o)/2$ is the Lindblad superoperator, and $J^- = \cos\theta \sigma_C^- + \sin\theta \sigma_B^-$ is the collective lowering operator. In what follows we mainly consider the range $0 < \theta < \pi/2$, and $\theta = \pi/4$ means that the couplings of the charger and the QB to the environment are the same.

Naturally, we hope the QB can be fully charged, which means the QB can be excited to the corresponding highest energy level. Nevertheless, the environment will stabilize the system into a mixed state, so it is difficult to achieve full charging in an open system. Our goal is to improve the stored energy of the QB as much as possible on the premise of stable charging, thus a quantum jump-based feedback control

is introduced to our system. This feedback operator can be added directly to the Eq. (5) by inserting a unitary operator before the collective lowering operator J^-. In the absence of time delay of the feedback control, and the whole system can be expressed by the Markovian master equation [55] (see Appendix A)

$$\dot{\rho} = \Gamma \mathcal{L}[U_{\text{fb}} J^-] \rho, \tag{6}$$

where $U_{\text{fb}} = \exp\{-i\lambda[(|g\rangle_C\langle e| + |e\rangle_C\langle g|) \otimes I_B]\delta t\}$ is the unitary operator of feedback control operating on the charger, and λ denotes the feedback strength, I_B is the identity operator of the QB. For the feedback to be Markovian, the mechanism must cause the system to change immediately and lead to a finite amount of evolution, which means that δt should be small and the feedback strength should be large relatively. By defining $\omega = \lambda \delta t$, we get $U_{\text{fb}} = \exp\{-i\omega[(|g\rangle_C\langle e| + |e\rangle_C\langle g|) \otimes I_B]\}$, and $\mathcal{L}[U_{\text{fb}} J^-]\rho = U_{\text{fb}} J^- \rho J^+ U_{\text{fb}}^\dagger - (J^+ J^- \rho + \rho J^+ J^-)/2$. The feedback control of the charger is triggered as the decay described by the collective operator J^- is detected.

At the time t, the energy of the charger and QB can be expressed as $E_{C(B)}(t) = \text{Tr}[H_{C(B)}\rho_{C(B)}(t)]$, where $\rho_{B(C)}(t)$ is the reduced density matrix for $\rho(t)$. The initial state of the system is $|e\rangle_C|g\rangle_B$, thus, $E_C(0) = \omega_0$ and $E_B(0) = 0$. To describe the energy transfer process, we define the energy change of the charger and the QB as

$$\Delta E_C(t) = E_C(t) - E_C(0), \tag{7}$$

$$\Delta E_B(t) = E_B(t) - E_B(0). \tag{8}$$

Note that $\Delta E_C(t)$ is always negative, since the initial time $E_C(0) = \omega_0$ and the charger energy decreases monotonously during charging. Thus, $|\Delta E_C(t)|$ means the energy released by the charger during the charging process, and $\Delta E_B(t)$ represents the stored energy of the QB during this process. When the QB is fully charged, the stored energy of the QB is $\Delta E_{B\text{full}} = \omega_0$. In addition, the charging power of the QB is defined as

$$P_B(t) = \frac{\Delta E_B(t)}{t}. \tag{9}$$

To find the optimal value of the feedback parameter ω, we solve the master equation of Eq. (6) and obtain a steady state that is related to the initial state of the system as

$$\rho^{ss} = \frac{-4\sin^4\theta}{-3 + \cos(2\theta) - 2\cos^2\theta\cos(2\omega)}|eg\rangle\langle eg|$$

$$+ \frac{-1 + \cos(4\theta)}{2[-3 + \cos(2\theta) - 2\cos^2\theta\cos(2\omega)]}|ge\rangle\langle ge|$$

$$+ \frac{4\cos^2\theta\cos^2\omega}{3 - \cos(2\theta) + 2\cos^2\theta\cos(2\omega)}|gg\rangle\langle gg|$$

$$+ \left\{ \frac{4\cos\theta\sin^3\theta}{-3 + \cos(2\theta) - 2\cos^2\theta\cos(2\omega)}|eg\rangle\langle ge| \right.$$

$$+ \frac{i\sin^2(2\theta)\sin(2\omega)}{2[-3 + \cos(2\theta) - 2\cos^2\theta\cos(2\omega)]}|eg\rangle\langle gg|$$

$$\left. + \frac{2i\cos^3\theta\sin\theta\sin(2\omega)}{3 - \cos(2\theta) + 2\cos^2\theta\cos(2\omega)}|ge\rangle\langle gg| + \text{H.c.} \right\}. \tag{10}$$

In the absence of feedback control, i.e., $\omega = 0$, the corresponding steady state of the system is

$$\rho^{ss} = \sin^2\theta|\psi_1\rangle\langle\psi_1| + \cos^2\theta|gg\rangle\langle gg|. \tag{11}$$

This steady state is a mixed state, where $|\psi_1\rangle = \sin\theta|e\rangle_C|g\rangle_B - \cos\theta|g\rangle_C|e\rangle_B$. Then, according to the Eqs. (7) and (8), we obtain

$$\Delta E_C(\infty) = \omega_0(\sin^4\theta - 1), \tag{12}$$

$$\Delta E_B(\infty) = \omega_0(\sin^2\theta - \sin^4\theta). \tag{13}$$

We can see clearly that $|\Delta E_C(\infty)| - \Delta E_B(\infty) = \omega_0\cos^2\theta > 0$, which means that only a portion of the energy released by the charger is transferred to the QB, and the rest is dissipated into the environment. In addition, the stored energy of the QB in the steady state is $\Delta E_B(\infty) = \omega_0(\sin^2\theta - \sin^4\theta) = \sin^2(2\theta)/4$, which can reach its maximum $\Delta E_B(\infty) = 0.25\omega_0$ as the coupling strengths of charger and QB to the environment are the same, i.e., $\theta = \pi/4$.

On the contrary, when the feedback control is switched on, i.e., $\omega \neq 0$, we have

$$\Delta E_C(\infty) = \frac{4\omega_0\sin^4\theta}{4 - [1 - \cos(2\omega)][\cos(2\theta) + 1]} - 1, \tag{14}$$

$$\Delta E_B(\infty) = \frac{\omega_0\sin^2(2\theta)}{4 - [1 - \cos(2\omega)][\cos(2\theta) + 1]}. \tag{15}$$

When $\cos(2\omega) = -1$ for a fixed value of θ, the corresponding stored energy of QB is the maximum. Therefore, the optimal value of the feedback parameter is $\omega = 0.5\pi$. In this case, we find $\Delta E_B(\infty) = |\Delta E_C(\infty)| = \omega_0\cos^2\theta$, which means that the energy released by the charger is completely transferred to the QB, avoiding the waste of energy and improving the efficiency of energy transfer. The corresponding steady state is

$$\rho^{ss} = |\psi_1\rangle\langle\psi_1|. \tag{16}$$

This steady state shows that the feedback control can avoid the decay of the system into the double occupations of ground state. We observe that when $\cos\theta$ approaches 1, the charger is nearly fully discharged and the QB is nearly fully charged. But it is worth emphasizing that $\cos\theta \sim 1$ and $\cos\theta = 1$ are two different coupling conditions, which have completely different effects on the system. For $\cos\theta = 1$, by solving the master equation of Eq. (6) again, we obtain that the form of steady state is $\rho^{ss} = |gg\rangle\langle gg|$, which means no energy is stored in the QB. Therefore, the coupling strength between the QB and the environment is nonnegligible although it is weak as $\cos\theta$ approaches 1, and the corresponding feedback energy costs are discussed in Appendix C.

C. Numerical simulations

In Fig. 1, we plots the stored energy $\Delta E_B(\infty)/\omega_0$ of the QB in the steady state as a function of ω based on Eq. (6). Different curves correspond to different values of θ. The red dotted line describes the variation of stored energy $\Delta E_B(\infty)/\omega_0$ of the QB with the control parameter ω when the coupling strengths of charger and QB to the environment are the same ($\theta = \pi/4$). The green solid line, black dashed line

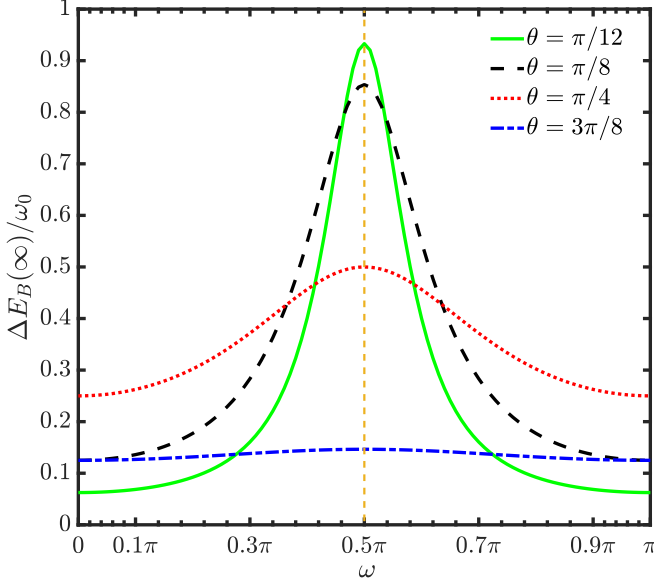FIG. 1. The energy stored in the QB at steady state, which is a function of ω with different θ. Different curves correspond to different values of θ, i.e., $\theta = \pi/12$ (green solid line), $\theta = \pi/8$ (black dashed line), $\theta = \pi/4$ (red dotted line), and $\theta = 3\pi/8$ (blue dash-dotted line).

and blue dash-dotted line describe the variation of stored energy $\Delta E_B(\infty)/\omega_0$ of the QB with ω when the charger and QB have different couplings, and the corresponding θ are $\pi/12$, $\pi/8$ and $3\pi/8$, respectively. As shown in Fig. 1, $\omega = 0.5\pi$ corresponds to the optimal value for the stored energy of the QB in steady state under different θ, which is consistent with our analytical results. We can also see that when the feedback control is switched off ($\omega = 0$), the stored energy of the QB in the steady state is optimal when the coupling strengths of charger and QB to the environment are the same. Obviously, the QB cannot be charged effectively in this situation. Once the charger and the QB have different coupling strengths, the charging effect becomes worse. However, in the presence of the feedback control ($\omega = 0.5\pi$), the $\Delta E_B(\infty)$ increases significantly as the value of θ decreases. Hence, the feed-

back control is beneficial to charge the QB, especially as the charger and QB have nonidentical couplings.

In Fig. 2(a) [2(b)] we plot $|\Delta E_c(t)|$ $[\Delta E_B(t)]$ of the charger (QB) as a function of Γt. The numerical analysis reveals that the energy is transferred from the charger to the QB via the environment, and we have $|\Delta E_C(\infty)| = \Delta E_B(\infty)$. The stored energy of QB in the steady state increases as the value of θ decreases, but the energy convergence time is prolonged. The charging power $P_B(t)$ is shown in Fig. 2(c), and the maximum charging power of QB decreases as the stored energy of the QB increases. In addition, when $\theta = 3\pi/8$, there is $\cos\theta < \sin\theta$, meaning that the couple strength between the QB and the environment (g_{Bk}) is greater than that between the charger and the environment (g_{Ck}). Combining with Figs. 2(b) and 2(c), the stored energy and power of the QB are lower in this case, which is not conducive to charging of the QB. Therefore, it is necessary to adjust the coupling strength to meet $g_{Ck} > g_{Bk}$, i.e., $\cos\theta > \sin\theta$ ($0 < \theta < \pi/4$) in the following discussion.

D. The ergotropy of the QB

Up to now, we have analyzed the stored energy of the QB under feedback control. It is worth noting that not all the energy stored in QB can be completely extracted. To quantify the maximum work extraction from the QB, we introduce the concept of ergotropy [66,67] that can be expressed by

$$\Sigma_B(t) = E_B(t) - E_p(t)$$
$$= \text{Tr}[H_B \rho_B(t)] - \min_U \text{Tr}[U \rho_B(t) U^\dagger H_B]. \quad (17)$$

The $E_p(t)$ represents the minimum energy locked in the QB, which cannot be extracted from the QB by an unitary evolution U. When the maximum work is extracted, the system will be left in the corresponding passive state [28,68,69]. For a passive state σ, one has $\Sigma_B(\sigma) = 0$, i.e., for all unitaries U to meet

$$\text{Tr}(\sigma H) \leqslant \text{Tr}(U \sigma U^\dagger H). \quad (18)$$

Now we calculate the ratio of ergotropy to the stored energy of QB at steady state. We discuss it in two cases here.
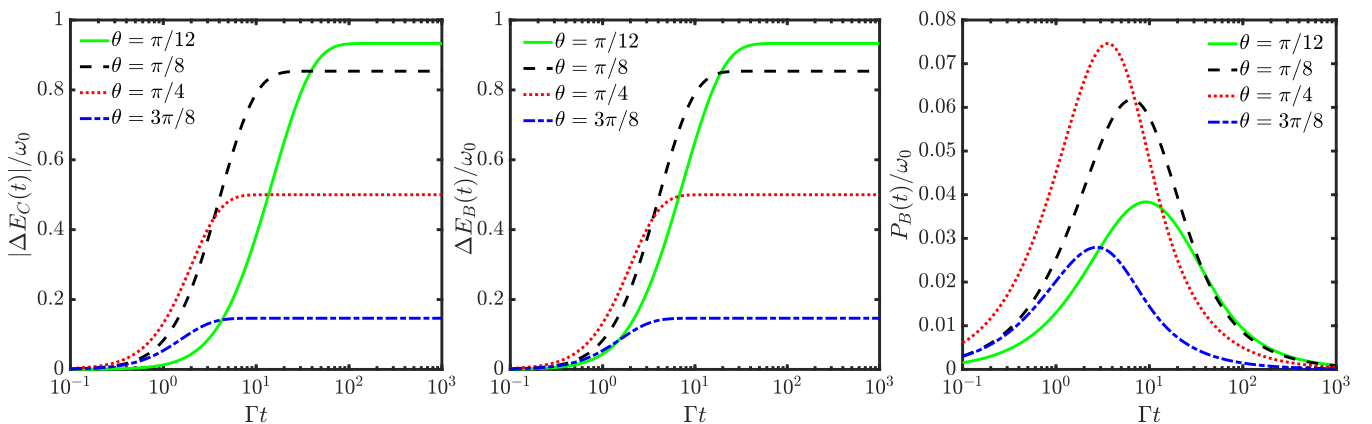

FIG. 2. (a) The released energy $|\Delta E_C(t)|$ of the charger as a function of Γt. (b) The stored energy $\Delta E_B(t)$ of the QB as a function of Γt. (c) The charging power $P_B(t)$ of the QB. Different curves correspond to different values of the θ. The green solid line: $\theta = \pi/12$; The black dashed line: $\theta = \pi/8$; The red dotted line: $\theta = \pi/4$; The blue dash-dotted line: $\theta = 3\pi/8$.
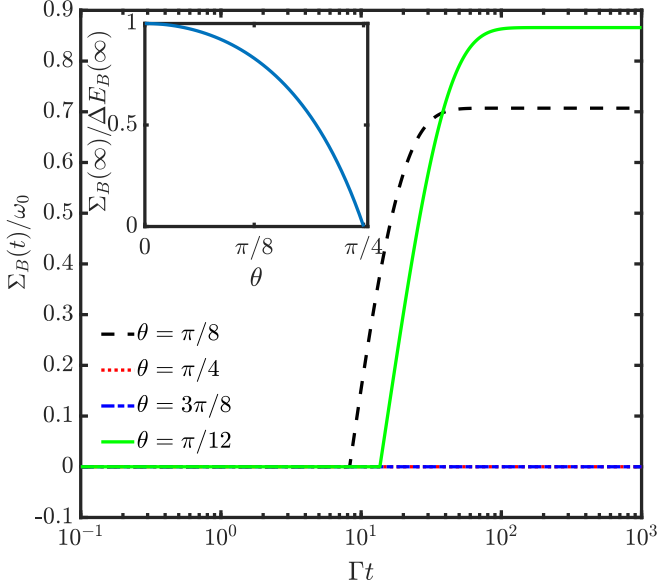
FIG. 3. The effect of coupling strength on ergotropy is studied. Different curves correspond to different θ. The green solid line corresponds to $\theta = \pi/12$, the black dashed line corresponds to $\theta = \pi/8$, the red dotted line corresponds to $\theta = \pi/4$ and the blue dash-dotted line corresponds to $\theta = 3\pi/8$. The inset is the ratio of ergotropy to energy stored in the QB at the steady state, which is a function of θ.

When $g_{Ck} > g_{Bk}$, i.e., $\cos\theta > \sin\theta$ ($0 < \theta < \pi/4$), according to Ref. [36], the ratio is expressed as

$$\frac{\Sigma_B(\infty)}{\Delta E_B(\infty)} = \frac{\omega_0(\cos^2\theta - \sin^2\theta)}{\omega_0\cos^2\theta} = 1 - \tan^2\theta. \qquad (19)$$

$\Sigma_B(\infty)/\Delta E_B(\infty) > 0$ means that the energy can be extracted from the QB, and the ergotropy tends to the stored energy of the QB gradually as the value of the θ decreases.

When $g_{Ck} \leqslant g_{Bk}$, i.e., $\cos\theta \leqslant \sin\theta$ ($\pi/4 \leqslant \theta < \pi/2$), the ratio is expressed as

$$\frac{\Sigma_B(\infty)}{\Delta E_B(\infty)} = \frac{\omega_0(\cos^2\theta - \cos^2\theta)}{\omega_0\cos^2\theta} = 0. \qquad (20)$$

In this case, no energy can be extracted from the QB, that is, the QB is in passive states. Thus, $\theta \in [\pi/4, \pi/2)$ is not conducive to the extraction of QB energy.

In Fig. 3, we plot the ergotropy $\Sigma_B(t)$ as a function of Γt, the green solid line, the black dashed line, the blue dash-dotted line, and the red dotted line correspond to the value of θ: $\pi/12$, $\pi/8$, $\pi/4$ and $3\pi/8$, respectively. Combined with Fig. 2(b) and Fig. 3, it can be easily seen that $\Sigma_B(t) < \Delta E_B(t)$ for a given value of θ, and the ergotropy increases as the value of the θ decreases and tends to the stored energy of the QB gradually. Moreover, a behavior can be observed that ergotropy keeps zero at some time intervals until $\Delta E_B(t) > 1/2$. According to Eq. (18), we can judge that the QB is in passive states during this period of time. Thus, no energy can be extracted from the QB. The inset characterizes the ratio of ergotropy to energy stored in the QB at the steady state, where we only consider $0 < \theta \leqslant \pi/4$. For details of calculating ergotropy is shown in Appendix D.
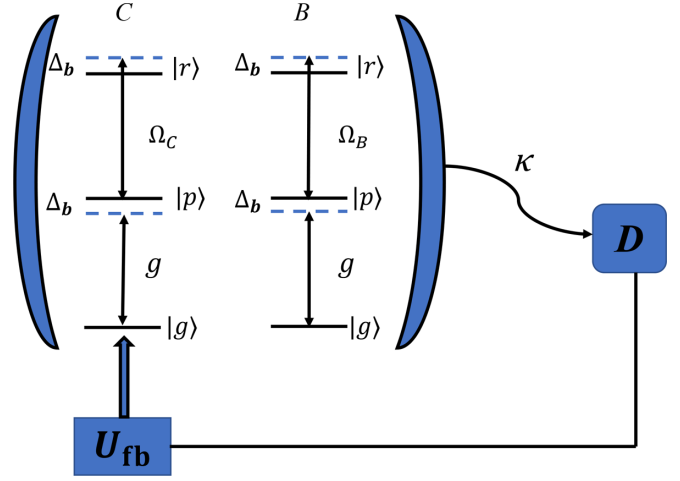

FIG. 4. The charger C and the QB B are described by identical Rydberg atoms with cascade-type configuration. Each of atoms contains a Rydberg state $|r\rangle$, an optical state $|p\rangle$, and a ground state $|g\rangle$. The intermediate state $|p\rangle$ can be eliminated adiabatically under the large-detuning condiation $|\Delta_b| \gg \Omega_{C(B)}$, which is then reduced to two effective two-level atom resonantly coupled to a damped optical cavity with coupling strength $g_{eff}^C = -g\Omega_C/\Delta_b$ and $g_{eff}^B = -g\Omega_B/\Delta_b$, respectively. The feedback control U_{fb} performed on the charger C is triggered right after the leakage photon is measured by the detector D.

III. IMPLEMENTATION OF THE PHYSICAL MODEL

A. Model description and system Hamiltonian

A natural question is whether the theoretical model described in Sec. II can be actually implemented in a physical system. In experiments, it is difficult to observe atomic collective decay. Therefore, in this part, we designed an equivalent physical scheme, which incorporates a dissipative cavity. When the signal of photon leakage of cavity field is detected, the feedback control of the charger is triggered, to realize stable and effective charging of the QB.

As shown in Fig. 4, the charger and the QB are described by identical Rydberg atoms with cascade-type configuration, respectively. Each of atoms contains a Rydberg state $|r\rangle$, an optical state $|p\rangle$ and a ground state $|g\rangle$. Initially, the QB is in ground state $|g\rangle$ and the charger is in Rydberg state $|r\rangle$. Meanwhile, the charger and the QB are coupled to the cavity mode with strength g, detuned by Δ_b, and pumped by two classical fields, respectively, the corresponding Rabi frequencies and detuning are denoted by $\Omega_{C(B)}$ and $-\Delta_b$. There are three main reasons for choosing the Rydberg atoms: First, the coupling strength of the charger (QB) to the cavity field can be controlled by adjusting the corresponding detuned Δ_b and Rabi frequency $\Omega_{C(B)}$. Second, the Rydberg atoms have stable excited states due to the low spontaneous decay rate. Last, the Rydberg atom with higher energy levels can store more energy, compared with other atomic systems. For convenience, we assume that all parameters are real. The total Hamiltonian is described as $H = H_0 + H_I$, where H_0 represents the free Hamiltonian of the system, and H_I represents the

interact Hamiltonian of the system. The corresponding forms are expressed as

$$H_0 = \sum_{i=C,B} \omega_g |g\rangle_i \langle g| + \omega_p |p\rangle_i \langle p| + \omega_r |r\rangle_i \langle r| + \omega_c a^\dagger a, \quad (21)$$

$$H_I = \sum_{i=C,B} ga|p\rangle_i \langle g| + \Omega_i e^{-i\omega_i t} |r\rangle_i \langle p| + \text{H.c.}$$
$$+ U_{CB}(r)|r\rangle_C \langle r| \otimes |r\rangle_B \langle r|, \quad (22)$$

where $\omega_g < \omega_p < \omega_r$. The Rydberg-mediated interaction $U_{CB}(r)$ is produced from the dipole-dipole potential of the scale C_3/r^3 or the long-range van der Waals interaction proportional to C_6/r^6, where r is the distance between two Rydberg atoms and $C_{3(6)}$ depends on the quantum numbers of the Rydberg state.

In the interaction picture, the Hamiltonian reads

$$H_{\text{int}} = \sum_{i=C,B} ge^{i\Delta_b t} a|p\rangle_i \langle g| + \Omega_i e^{-i\Delta_b t} |r\rangle_i \langle p| + \text{H.c.}$$
$$+ U_{CB}(r)|r\rangle_C \langle r| \otimes |r\rangle_B \langle r|, \quad (23)$$

where $\Delta_b = \omega_p - \omega_g - \omega_c = \omega_{C(B)} - \omega_r + \omega_p$. The evolution of the system is confined in the one-excitation subspace, so the Rydberg interaction term has no effect on our results, and we will ignore it in the following expressions. Under the condition of the large detuning, i.e., $|\Delta_b| \gg \{g, \Omega_{C(B)}\}$, the intermediate state $|p\rangle$ may be eliminated safely, and the interaction Hamiltonian can be reduced to

$$H_{\text{int}} = -\frac{g^2 a^\dagger a}{\Delta_b}|g\rangle_C \langle g| - \frac{\Omega_C}{\Delta_b}|r\rangle_C \langle r|$$
$$-\frac{g^2 a^\dagger a}{\Delta_b}|g\rangle_B \langle g| - \frac{\Omega_B}{\Delta_b}|r\rangle_B \langle r|$$
$$-\left[\frac{ga\Omega_C}{\Delta_b}|r\rangle_C \langle g| + \frac{ga\Omega_B}{\Delta_b}|r\rangle_B \langle g| + \text{H.c.}\right]. \quad (24)$$

The first two terms are on behalf of the Stark shifts of ground states and Rydberg states, respectively, which can be canceled by the introduction of other auxiliary levels. Therefore, the above Hamiltonian is simplified to be

$$H_{\text{eff}} = \sum_{i=B,C} g_{\text{eff}}^j |r\rangle_i \langle g| a + \text{H.c.}, \quad (25)$$

where $g_{\text{eff}}^C = -g\Omega_C/\Delta_b$ ($g_{\text{eff}}^B = -g\Omega_B/\Delta_b$) is the effective coupling strength between the charger (QB) and the cavity mode. We can clearly see that both the charger C and the QB B are equivalent to atoms with two-level structure. The reason why we do not directly choose atoms with two-level configurations is that the cascade atoms is more advantageous in term of the feasibility of experiment [70–73], and the effective coupling strength can be controlled by adjusting the corresponding detunings and Rabi frequencies.

According to the simplified Hamiltonian, we can obtain three eigenstates: $|E_0\rangle = \sin\theta|rg\rangle|0\rangle - \cos\theta|gr\rangle|0\rangle$, $|E_-\rangle = (\cos\theta|rg\rangle|0\rangle + \sin\theta|gr\rangle|0\rangle - |gg\rangle|1\rangle)/\sqrt{2}$, and $|E_+\rangle = (\cos\theta|rg\rangle|0\rangle + \sin\theta|gr\rangle|0\rangle + |gg\rangle|1\rangle)/\sqrt{2}$, the corresponding eigenvalues are $E_0 = 0$, $E_- = -g\Omega_R/\Delta_b$ and $E_+ = g\Omega_R/\Delta_b$, respectively, in which $\Omega_R^2 = \Omega_C^2 + \Omega_B^2$, and $\theta = \arctan[\Omega_B/\Omega_C] \in (0, \pi/2)$.

B. Master equation based on feedback with negligible time delay

In the absence of feedback control, considering the influence of dissipation at a low temperature mechanism ($T = 0$), the evolution of the system is governed by

$$\dot{\rho} = -i[H_{\text{eff}}, \rho] + \mathcal{L}_\kappa \rho + \mathcal{L}_\gamma \rho, \quad (26)$$

where $\mathcal{L}_\kappa \rho = \kappa/2(2a\rho a^\dagger - a^\dagger a\rho - \rho a^\dagger a)$, $\mathcal{L}_\gamma \rho = \Sigma_{i=B,C} \gamma/2(2\sigma_i^- \rho\sigma_i^+ - \sigma_i^+ \sigma_i^- \rho - \rho\sigma_i^+ \sigma_i^-)$, κ is the decay rate of the cavity mode, γ is the spontaneous rate of the Rydberg state, and $\sigma_i^- = (\sigma_i^+)^\dagger$ is the lowing operator of the charger (QB). In the single excitation regime, the above Lindblad master equation is reduced to

$$\dot{\rho} = -ig_{\text{eff}}[(J^+ a + J^- a^\dagger), \rho] + \mathcal{L}_\kappa \rho + \mathcal{L}_\gamma \rho, \quad (27)$$

where we have introduced $g_{\text{eff}} = -g\Omega_R/\Delta_b$. Therefore, we can reformulate the expressions for g_{eff}^C and g_{eff}^B as $g_{\text{eff}}^C = g_{\text{eff}} \cos\theta$ and $g_{\text{eff}}^B = g_{\text{eff}} \sin\theta$, and the corresponding collective lowing operator is scaled by $J^- = \sum_{i=C,B} g_{\text{eff}}^i/g_{\text{eff}} |g\rangle_i \langle r|$.

To understand the dissipative dynamics of the system more thoroughly, we use the number of photons to express the master equation of Eq. (27) [62]. In the limit $\kappa \gg g_{\text{eff}}$, by adiabatically eliminate the cavity mode, we finally get the reduced master equation of the system (see Appendix E),

$$\dot{\rho} = \Gamma \mathcal{L}[J^-]\rho + \mathcal{L}_\gamma \rho, \quad (28)$$

where $\Gamma = 4g_{\text{eff}}^2/\kappa$ is the collective amplitude damping rate of the transition from $|r\rangle$ to $|g\rangle$. If the collective decay rate is much large than the spontaneous emission rate, i.e., $\Gamma \gg \gamma$, then an effective master equation can be expressed as

$$\dot{\rho} = \Gamma \mathcal{L}[J^-]\rho. \quad (29)$$

When the quantum feedback control is applied to the charger, the effective master equation of the system reads

$$\dot{\rho} = \Gamma \mathcal{L}[U_{\text{fb}} J^-]\rho, \quad (30)$$

now we recover the result with the same form as Eq. (6), where $J^- = \cos\theta|g\rangle_C \langle r| + \sin\theta|g\rangle_B \langle r|$.

In experiments, the actual signal does not come from the collective damping of the atoms, but from the photons leaking out of the cavity mode. Therefore, we consider a more realistic feedback master equation,

$$\rho = -ig_{\text{eff}}[(J^+ a + J^- a^\dagger), \rho] + \kappa \mathcal{L}[U_{\text{fb}} a]\rho. \quad (31)$$

By applying an adiabatic elimination to the above master equation, this system can be effectively described in the collective spin basis, as shown in the master equation of Eq. (29). For a discussion of the finite temperatures, please see Appendix F for details.

The following numerical simulation is based on Eq. (31). Figures 5(a) and 5(b) represent the energy change of the charger and the QB, respectively, and Fig. 5(c) represents the charging power of the QB, where $\omega = 0.5\pi$, $\kappa = 25\Gamma$, $g_{\text{eff}} = 2.5\Gamma$, and we consider four-photon excitation in the cavity mode ($N_c = 5$). We observe that the physical model is in a good agreement with the theoretical results illustrated in the Sec. II. In addition, to obtain the analytical solution, we assume that $\kappa \gg g_{\text{eff}}$ to derive the effective master equation of Eq. (29). Nevertheless, in the Fig. 6, we find that κ does not have to be much greater than g_{eff} in numerical simulation.
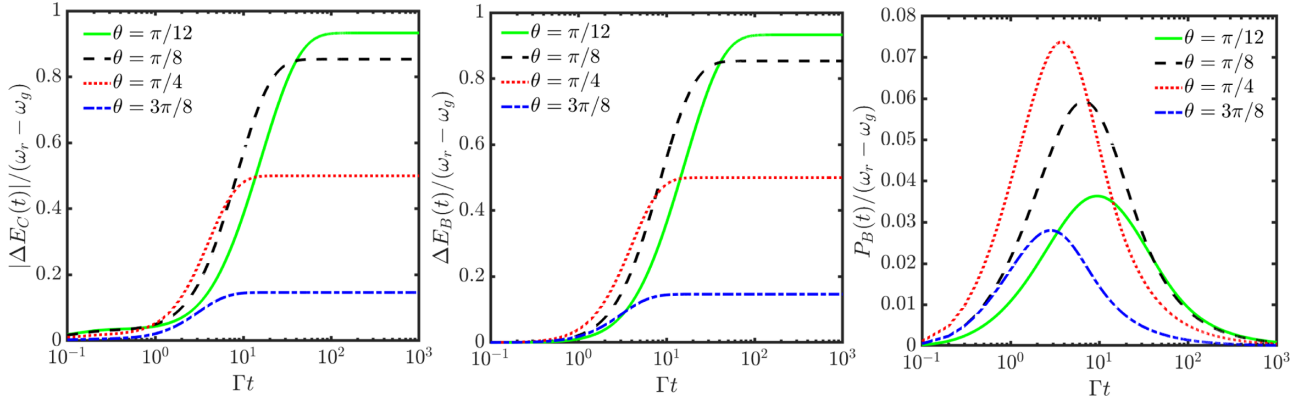
FIG. 5. Panels (a–c) describe the effects of different coupling strengths on the energy of the charger and the energy of the QB, as well as the charging power of the QB, in term of the Eq. (31). Different curves correspond to different θ. The dimension of cavity mode is $N_c = 5$, and the other parameters are $\kappa = 25\Gamma$ and $g_{\text{eff}} = 2.5\Gamma$.

At the same time, we find that there is no necessary to expand the dimension of the cavity to $N_c = 5$, since $N_c = 2$ is exact enough to describe our physical picture. In the following discussion, we only choose $N_c = 2$ if there is no special description.

Figure 7(a) displays the time evolution of the variance $\sigma_B = \sqrt{\langle H_B^2 \rangle - \langle H_B \rangle^2}$ of the QB energy, which measures the quality of the stored energy. A variance usually means that the energy provided by the QB has a fluctuation around its average energy. A large energy fluctuation represents that the amount of stored energy is highly sensitive to charging time, therefore it is difficult to estimate the amount of stored energy. The red solid line describes the variance of the QB when the charger and the QB have the same effective coupling

($\theta = \pi/4$), and the blue dashed line indicates that the two have different effective coupling strength ($\theta = \pi/8$). It can be clearly seen that when the effective coupling strengths are different, the stored energy quality of QB is better

C. The effect of a small time delay

So far, we have only discussed the effect of feedback control on the energy stored of the QB when there is no feedback time delay. This mechanism requires that the system changes immediately once the detector detects the leakage of photons from the cavity field. Thus, the corresponding master equation is a instantaneous feedback master equation. However, there is a time delay in the actual feedback control due to the limited response time of the device. In this part, we investigated the effect of feedback time delay on the energy storage of QB.
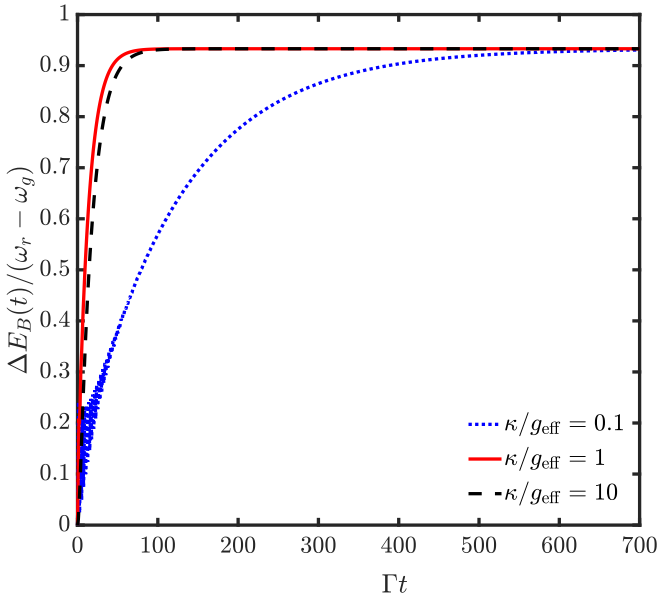

FIG. 6. Energy stored $\Delta E_B(t)$ as a function of Γt with different κ/g_{eff}. Different curves correspond to different κ/g_{eff} values. The blue dotted line: $\kappa/g_{\text{eff}} = 0.1$; The red solid line:$\kappa/g_{\text{eff}} = 1$; The blue dotted line: $\kappa/g_{\text{eff}} = 10$; The dimension of cavity mode is $N_c = 5$. Other parameters are given as $\theta = \pi/12$ and $\omega = 0.5\pi$.
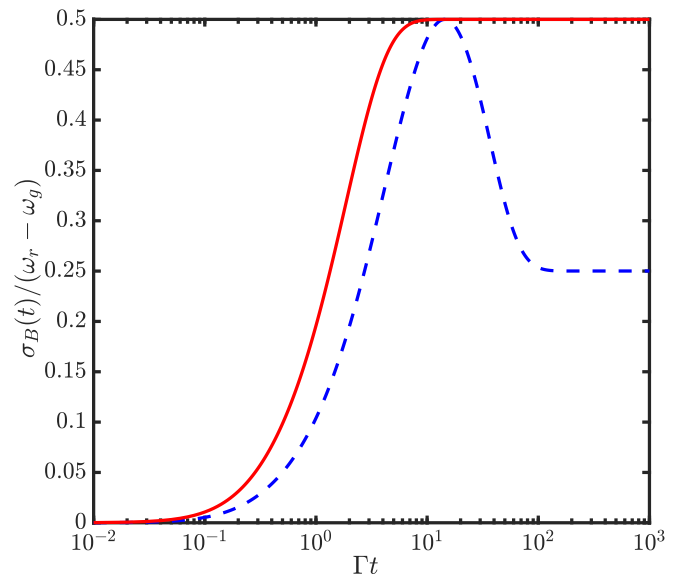

FIG. 7. Time evolution of the variance $\sigma_B = \sqrt{\langle H_B^2 \rangle - \langle H_B \rangle^2}$ of the QB energy. The red solid line: $\theta = \pi/4$; The blue dashed line: $\theta = \pi/8$. The other parameters are given as $\omega = 0.5\pi$, $\kappa = 25\Gamma$, and $g_{\text{eff}} = 2.5\Gamma$.
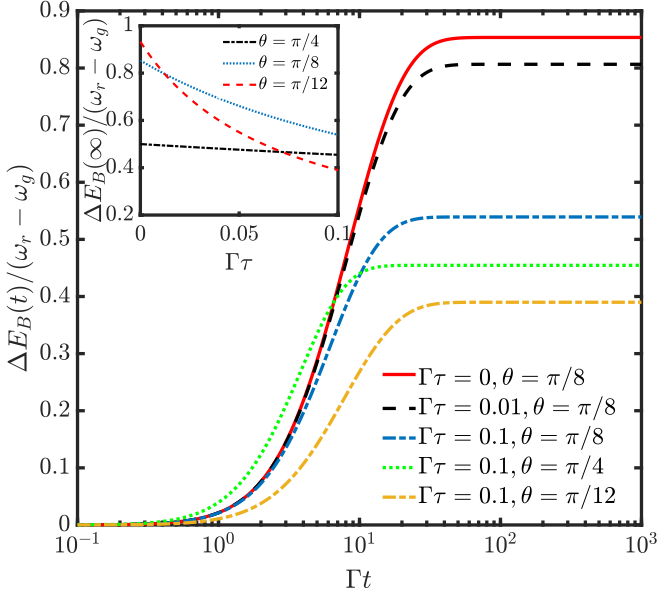
FIG. 8. The stored energy of the QB as a function of Γt governed by the master equation of Eq. (31) with delayed feedback control. The corresponding parameters are given as $\omega = 0.5\pi$, $\kappa = 25\Gamma$, and $g_{\rm eff} = 2.5\Gamma$. The inset is the stored energy in the QB at the steady state, which is a function of $\Gamma\tau$ with different θ.

The form of the master equation is [55] (see Appendix G)

$$\dot{\rho} = [\mathcal{D} + \tau(e^{\mathcal{K}} - 1)\{\mathcal{D}\mathcal{J}[a] - \mathcal{J}[a]\mathcal{D}\}]\rho, \qquad (32)$$

where $\mathcal{K}$ is a Liouville superoperator, in a special case, $\mathcal{K}\rho = -i[\omega[(|g\rangle_C\langle r| + |r\rangle_C\langle g|) \otimes I_B], \rho]$, $\mathcal{D}\rho \equiv -ig_{\rm eff}[(J^+a + J^-a^\dagger), \rho] + \kappa\mathcal{L}[U_{\rm fb}a]\rho$, and $\mathcal{J}[a]\rho = a\rho a^\dagger$. This master equation is equal to the instantaneous feedback master Eq. (31), plus a correction linear in τ. Obviously, when

$$\tau\|(e^{\mathcal{K}} - 1)\{\mathcal{D}\mathcal{J}[a] - \mathcal{J}[a]\mathcal{D}\}\rho\| \ll \|\mathcal{D}\rho\|, \qquad (33)$$

this correction to the Markovian feedback master equation can be negligible, where the $\|\|$ indicates a suitable norm (e.g., 1-norm, 2-norm, or ∞-norm).

In Fig. 8, we take into account the feedback time delay and plot the energy stored in the QB with different time delays $\Gamma\tau$. These results show that the energy stored in the QB decreases with the increase of $\Gamma\tau$. In this case, the presence of feedback delay increases the impact of dissipation on the energy storage of QB, leading to deviations from previous results. For example, the inset shows that for $\theta = \pi/12$, once $\Gamma\tau$ exceeds the critical value 0.012, the stored energy of the QB is lower than that for $\theta = \pi/8$. When this value is further greater than 0.072, the stored energy of the QB is not as good as the case for $\theta = \pi/4$.

D. The effect of the spontaneous emission

In the above discussion, we have ignored the spontaneous emission of the system. In this part, we will consider the influence of the spontaneous emission of the system on our scheme. The dynamics of the system governed by a time-

dependent master equation is given by

$$\dot{\rho} = -i[H_{\rm I}, \rho] + \sum_i \frac{\gamma_r}{2}\mathcal{L}[|p\rangle_i\langle r|]\rho + \sum_i \frac{\gamma_r}{2}\mathcal{L}[|g\rangle_i\langle r|]\rho$$

$$+ \sum_i \gamma_p\mathcal{L}[|g\rangle_i\langle p|]\rho + \kappa\mathcal{L}[U_{\rm fb}a]\rho, \qquad (34)$$

where $H_{\rm I}$ is the full Hamiltonian of Eq. (23). There are continuous decay mechanisms $|r\rangle \to |p\rangle$ and $|p\rangle \to |g\rangle$. Meanwhile, there is a discontinuous decay mechanisms from $|r\rangle$ to $|g\rangle$. For simplicity, we have assumed the decay rates of the atom from level $|r\rangle$ to $|p\rangle$ and $|r\rangle$ to $|g\rangle$ are the same. In general, the decay rate of the Rydberg state γ_r is three orders of magnitude lower than that of the intermediate state γ_p, and the effect of spontaneous emission of $|p\rangle$ can be further reduced by enlarging the value of detuning Δ_b, but at the cost of extending the convergence time and amplifying the effect of spontaneous emission of $|r\rangle$. So the tradeoff between γ_r and γ_p should be considered according to different parameters of the system. Based on the above results, we may exploit the recent cavity QED system with Rydberg atoms as a natural platform to realize our QB model [74–78]. We choose the configuration of ^{87}Rb atom for both the charger and the QB, the ground state of the battery is $5S_{1/2}$, the optical state is $5P_{3/2}$. The decay rates of the intermediate state $|p\rangle$ and the cavity mode are $\gamma_p = 2\pi \times 3$ MHz and $\kappa = 2\pi \times 0.66$ MHz, respectively. The optical level is coupled to the quantized cavity mode with strength $g = 2\pi \times 14.4$ MHz. We modulate the Rabi frequency of the classical field as $\Omega_C = 3g\cos\pi/8$ and $\Omega_B = 3g\sin\pi/8$. To resist the spontaneous emission of intermediate state $|p\rangle$, we set the single-photon detuning $\Delta_b = 160g$. The different Rydberg excited states can be utilized corresponding to different spontaneous decay rates, i.e., $\gamma_r = 2\pi \times 0.28$ kHz ($n = 80$) and $\gamma_r = 2\pi \times 0.14$ kHz ($n = 100$). Figure 9 shows the effect of different Rydberg states on the energy stored of the QB. There is no doubt that the Rydberg state with a large principal quantum number n has a better energy storage effect, which provides a battery energy storage value close to the ideal situation depicted in Fig. 8.

E. Multiparticle quantum barriers

In previous works, the charging effect of the multibody QBs had been explored. For instance, Ferraro et al. [19] proposed a Dicke QBs model in a closed system that N two-level systems interact with a single mode cavity field. In the numerical simulation, introducing a cutoff on the maximum number N_{ph} of photons, they had checked that excellent numerical convergence was achieved by choosing $N_{ph} = 4N$. Then they got a conclusion: The average charging power of a Dicke QBs is $\sqrt{N}$ times large than that of a single QB. Quach and Munro proposed an open QBs model [53], in which the charger and QB are composed of a spin ensemble, respectively, and the number of spins in the charger is greater than that of QBs. This work proved that the power density actually scales with the of number of spins N in the QBs. Both schemes, in a word, show that the exploitation of collective quantum resources can increase the charging power of QBs. In our work, we briefly analyze the impact of multiparticle QBs on energy transmission. The charger only contains a Rydberg atom while the
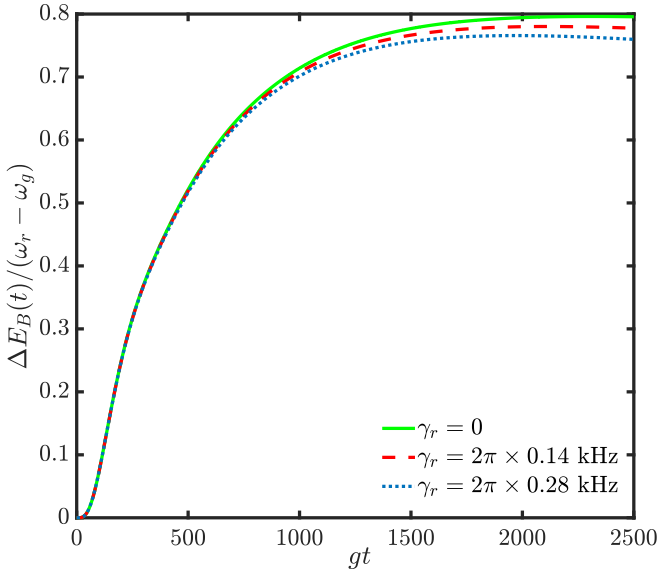
FIG. 9. The stored energy $\Delta E_B(t)$ of the QB as a function of gt. Different curves correspond to the spontaneous emission rate of the different Rydberg states, $\gamma_r = 0$ (green solid line), $\gamma_r = 2\pi \times 0.14$ kHz (red dashed line), and $\gamma_r = 2\pi \times 0.28$ kHz (blue dotted line). The dimension of cavity mode is $N_c = 5$ and the feedback parameter is $\omega = 0.5\pi$, other parameters are given as $\kappa = 2\pi \times 0.66$ MHz, $\gamma_p = 2\pi \times 3$ MHz, $g = 2\pi \times 14.4$ MHz, $\Omega_C = 3g\cos\pi/8$, $\Omega_B = 3g\sin\pi/8$, and $\Delta_b = 160g$.

QBs are made up of N atoms, where $N = 1 \sim 6$. According to Eq. (31) with $J^- = g_{eff}^C/g_{eff}|g\rangle\langle r| + \sum_{i=1}^{N} g_{eff}^B/g_{eff}|g\rangle_i\langle r|$, the energy stored by the multiparticle QBs is shown in Fig. 10(a) and the corresponding instantaneous charging power shows in Fig. 10(b). The corresponding parameters are $\omega = 0.5\pi$, $\theta = \pi/12$, $g_{eff} = 2.5\Gamma$, and $\kappa = 25\Gamma$. In addition, the dimension

of the cavity mode is set as $N_c = 2$. On the basis of Fig. 10, we find that as the number of atoms in the QBs increases, the maximum charging power of the QBs also increases, but the energy stored in the QBs decrease.

IV. SUMMARY

In summary, we have constructed a theoretical model for charging and stabilizing of the QB in an open system. The introductions of quantum feedback control and nonidentical coupling are conducive to the energy storage and ergotropy of QB. This model can be simulated in a Rydberg-cavity QED system, where the cascade Rydberg atom has the advantages of high energy storage, long lifetime, and adjustable coupling strength with cavity. We hope that the work will provide a valuable reference for future QB research.

APPENDIX A: DERIVATION OF QUANTUM MASTER EQUATIONS OF EQS. (5) AND (6)

In this Appendix, we give a simple derivation of the Eqs. (5) and (6). In the interaction picture, the Hamiltonian becomes

$$
\begin{aligned}
H_{int} = &\sum_k g_{Ck}[a_k^\dagger \sigma_C^- e^{-i(\omega_0 - \omega_k)t} + a_k \sigma_C^+ e^{i(\omega_0 - \omega_k)t}] \\
&+ \sum_k g_{Bk}[a_k^\dagger \sigma_B^- e^{-i(\omega_0 - \omega_k)t} + a_k \sigma_B^+ e^{i(\omega_0 - \omega_k)t}], \quad (A1)
\end{aligned}
$$

where g_{ik} $(i = C, B)$ is the coupling constant between the kth mode in the reservoir and the charger (QB).
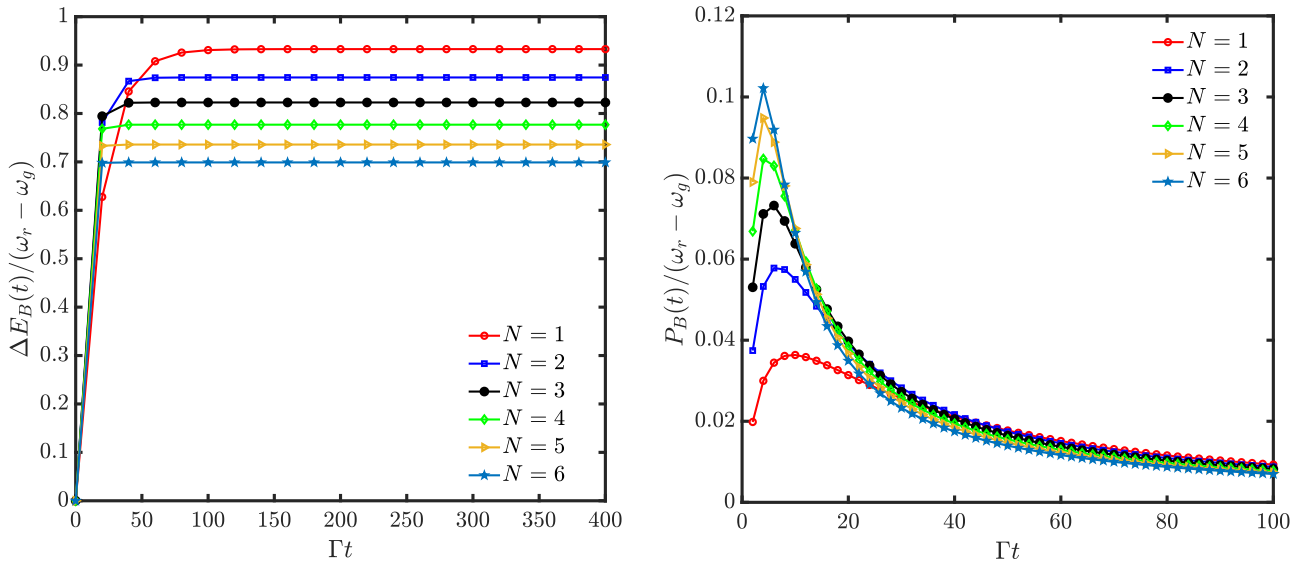

FIG. 10. (a) The local energy $\Delta E_B(t)$ of the QBs as a function of Γt. Different colors represent different numbers of particles in the QBs. The curves from top to bottom corresponds to $N = 1 \sim 6$. Panel (b) represents the charging power $P_B(t)$ of the QBs, however, the curves from top to bottom correspond to $N = 6 \sim 1$. All results in panels (a, b) have been obtained under the quantum feedback control ($\omega = 0.5\pi$). Other parameters are given as $\kappa = 25\Gamma$, $g_{eff} = 2.5\Gamma$, and $\theta = \pi/12$.

For convenience, we introduce $g_k = (g_{Ck}^2 + g_{Bk}^2)^{1/2}$. Therefore, $g_{Ck} = g_k g_{Ck}/(g_{Ck}^2 + g_{Bk}^2)^{1/2} = g_k \cos\theta$ and $g_{Bk} = g_k g_{Bk}/(g_{Ck}^2 + g_{Bk}^2)^{1/2} = g_k \sin\theta$. Subsequently, H_{int} can be rewritten as

$$H_{\text{int}} = \sum_k g_k \cos\theta [a_k^\dagger \sigma_C^- e^{-i(\omega_0 - \omega_k)t} + a_k \sigma_C^+ e^{i(\omega_0 - \omega_k)t}]$$
$$+ \sum_k g_k \sin\theta [a_k^\dagger \sigma_B^- e^{-i(\omega_0 - \omega_k)t} + a_k \sigma_B^+ e^{i(\omega_0 - \omega_k)t}]).$$

$$(A2)$$

Then we define $J^- = \cos\theta \sigma_C^- + \sin\theta \sigma_B^-$, and H_{int} is reduced to

$$H_{\text{int}} = \sum_k g_k [a_k^\dagger J^- e^{-i(\omega_0 - \omega_k)t} + a_k J^+ e^{i(\omega_0 - \omega_k)t}]. \quad (A3)$$

Under the Born-Markov approximation, the master equation reads

$$\dot{\rho}_S = -\text{Tr}_R \int_0^\infty d\tau [H_{\text{int}}(t), [H_{\text{int}}(t - \tau), \rho_S \otimes \rho_R]], \quad (A4)$$

where Tr_R stands for tracing over the degrees of freedom of the reservoir, ρ_R represents the density operator of the common reservoir and ρ_S represents the reduced density operator of the charger and the QB. In the following derivation, we use ρ instead of ρ_S for simplicity.

By combining the Eqs. (A3) and (A4), we can obtain the master equation of Eq. (5) as

$$\dot{\rho} = \Gamma \mathcal{L}[J^-]\rho, \quad (A5)$$

where $\Gamma \rightarrow \int_0^t dt' \sum_k g_k^2 e^{\pm(\omega_0 - \omega_k)(t-t')}$ and $\mathcal{L}[o] \equiv o\rho o^\dagger - (o^\dagger o\rho + \rho o^\dagger o)/2$. If both the charger and the QB are made up of an atomic ensemble, then the above master equation still holds, in which $J^- = J_C^- + J_B^- = \cos\theta \sum_{j=1}^N \sigma_{Cj}^- + \sin\theta \sum_{j=1}^N \sigma_{Bj}^-$.

Reference [55] points out that for the feedback to be Markovian, the mechanism must act immediately after a detection and cause a finite amount evolution of the system. This finite evolution is influenced by the superoperator $e^{\mathcal{K}}$, where $\mathcal{K}$ is a Liouville superoperator. To understand quantum feedback dynamics concisely, superoperator $\mathcal{L}[J^-]\rho$ is divided into two parts. The form is $\mathcal{L}[J^-]\rho = \mathcal{J}[J^-]\rho - \mathcal{A}[J^-]\rho$, in which $\mathcal{J}[J^-]\rho = J^-\rho J^+$ and $\mathcal{A}[J^-]\rho = [J^+ J^-\rho + \rho J^+ J^-]/2$. Due to $\mathcal{A}[J^-]\rho$ indicates a null measurement, leading the density operator $\tilde{\rho}_0(t + dt)$ unchanged, the density operator following a detection at time t is

$$\tilde{\rho}_1(t + dt) = e^{\mathcal{K}} J^- \rho J^+ dt. \quad (A6)$$

Then, the master equation of the system can be written as

$$\dot{\rho} = e^{\mathcal{K}} \mathcal{J}[J^-]\rho + \mathcal{A}[J^-]\rho, \quad (A7)$$

in the case that $\mathcal{K}\rho = -i[z, \rho]$, the master equation is simplified to

$$\dot{\rho} = \mathcal{L}[U_{\text{fb}} J^-]\rho, \quad (A8)$$

where $U_{\text{fb}} = e^{-iz}$ is the feedback control unitary operator operating on the system. Notably, the choice of the z is particularly important for our system. The previous work shows that the principle of choosing feedback control is to break the

symmetry of atomic exchange. Thus, the feedback operator is expressed as $U_{\text{fb}} = \exp\{-i\lambda[(|g\rangle_C\langle e| + |e\rangle_C\langle g|) \otimes I_B]\delta t\}$ in our work, where λ denotes the feedback strength, I_B is the identity operator of the QB. Then by defining $\omega = \lambda\delta t$, U_{fb} can be rewritten as $U_{\text{fb}} = \exp\{-i\omega[(|g\rangle_C\langle e| + |e\rangle_C\langle g|) \otimes I_B]\}$. Equation (6) shows that when the decay described by the collective operator J^- is observed, the mechanism causes the system to immediately change according to the measurement result.

APPENDIX B: DERIVATION OF THE STEADY STATE OF THE SYSTEM

To obtain the dynamics of state ρ at an arbitrary time t, we use a basis set as $|1\rangle = |e\rangle_C|e\rangle_B$, $|2\rangle = |e\rangle_C|g\rangle_B$, $|3\rangle = |g\rangle_C|e\rangle_B$, and $|4\rangle = |g\rangle_C|g\rangle_B$ to represent the density matrix as

$$\rho(t) = \begin{pmatrix} \rho_{11}(t) & \rho_{12}(t) & \rho_{13}(t) & \rho_{14}(t) \\ \rho_{21}(t) & \rho_{22}(t) & \rho_{23}(t) & \rho_{24}(t) \\ \rho_{31}(t) & \rho_{32}(t) & \rho_{33}(t) & \rho_{34}(t) \\ \rho_{41}(t) & \rho_{42}(t) & \rho_{43}(t) & \rho_{44}(t) \end{pmatrix}. \quad (B1)$$

According to the initial conditions $\rho_{22}(0) = 1$, we first calculate the system of equations composed of $\dot{\rho}_{1i}(t)$ ($i = 1 \sim 4$) and $\dot{\rho}_{j1}(t)$ ($j = 1 \sim 4$), and we get the solutions $\rho_{1i}(t) = \rho_{j1}(t) = 0$. Therefore, the remaining differential equations can be reduced to

$$\dot{\rho}_{22}(t) = \Gamma\{\sin^2\omega\cos^2\theta\rho_{22}(t) + \sin^2\omega\sin^2\theta\rho_{33}(t)$$
$$+ \sin^2\omega\sin\theta\cos\theta[\rho_{32}(t) + \rho_{23}(t)]\}$$
$$- \frac{\Gamma}{2}\{\sin\theta\cos\theta[\rho_{32}(t) + \rho_{23}(t)]$$
$$+ 2\cos^2\theta\rho_{22}(t)\}, \quad (B2)$$

$$\dot{\rho}_{33}(t) = -\frac{\Gamma}{2}\{\sin\theta\cos\theta[\rho_{32}(t) + \rho_{23}(t)]$$
$$+ 2\sin^2\theta\rho_{33}(t)\}, \quad (B3)$$

$$\dot{\rho}_{44}(t) = \Gamma\{\cos^2\omega\cos^2\theta\rho_{22}(t) + \cos^2\omega\sin^2\theta\rho_{33}(t)$$
$$+ \cos^2\omega\sin\theta\cos\theta[\rho_{32}(t) + \rho_{23}(t)]\}, \quad (B4)$$

$$\dot{\rho}_{23}(t) = -\frac{\Gamma}{2}\{\cos^2\theta\rho_{23}(t) + \sin\theta\cos\theta[\rho_{33}(t) + \rho_{22}(t)]$$
$$+ \sin^2\theta\rho_{23}(t)\}, \quad (B5)$$

$$\dot{\rho}_{24}(t) = -i\Gamma\{\sin\omega\cos\omega[\cos^2\theta\rho_{22}(t) + \sin^2\theta\rho_{33}(t)]$$
$$+ \sin\omega\cos\omega\cos\theta\sin\theta[\rho_{32}(t) + \rho_{23}(t)]\}$$
$$- \frac{\Gamma}{2}[\cos^2\theta\rho_{24}(t) + \cos\theta\sin\theta\rho_{34}], \quad (B6)$$

$$\dot{\rho}_{32}(t) = -\frac{\Gamma}{2}\{\cos^2\theta\rho_{32}(t) + \sin\theta\cos\theta[\rho_{33}(t) + \rho_{22}(t)]$$
$$+ \sin^2\theta\rho_{32}(t)\}, \quad (B7)$$

$$\dot{\rho}_{34}(t) = -\frac{\Gamma}{2}[\sin^2\theta\rho_{34}(t) + \sin\theta\cos\theta\rho_{24}(t)], \quad (B8)$$

$$\dot{\rho}_{42}(t) = i\Gamma\{\sin\omega\cos\omega[\cos^2\theta\rho_{22}(t) + \sin^2\theta\rho_{33}(t)]$$
$$+ \sin\omega\cos\omega\cos\theta\sin\theta[\rho_{32}(t) + \rho_{23}(t)]\}$$

$$-\frac{\Gamma}{2}[\cos^2\theta \rho_{42}(t) + \cos\theta \sin\theta \rho_{43}], \quad \text{(B9)}$$

$$\dot{\rho}_{43}(t) = -\frac{\Gamma}{2}[\sin^2\theta \rho_{43}(t) + \sin\theta \cos\theta \rho_{42}(t)]. \quad \text{(B10)}$$

Then we can get the solutions of a series of time-dependent equations. By choosing the time to approach infinity, we obtain the steady state that is related to the initial state of the system, which is expressed as

$$\rho^{ss} = \frac{-4\sin^4\theta}{-3 + \cos(2\theta) - 2\cos^2\theta \cos(2\omega)}|eg\rangle\langle eg|$$

$$+\frac{-1 + \cos(4\theta)}{2[-3 + \cos(2\theta) - 2\cos^2\theta \cos(2\omega)]}|ge\rangle\langle ge|$$

$$+\frac{4\cos^2\theta \cos^2\omega}{3 - \cos(2\theta) + 2\cos^2\theta \cos(2\omega)}|gg\rangle\langle gg|$$

$$+\left\{\frac{4\cos\theta \sin^3\theta}{-3 + \cos(2\theta) - 2\cos^2\theta \cos(2\omega)}|eg\rangle\langle ge|\right.$$

$$+\frac{i\sin^2(2\theta)\sin(2\omega)}{2[-3 + \cos(2\theta) - 2\cos^2\theta \cos(2\omega)]}|eg\rangle\langle gg|$$

$$+\left.\frac{2i\cos^3\theta \sin\theta \sin(2\omega)}{3 - \cos(2\theta) + 2\cos^2\theta \cos(2\omega)}|ge\rangle\langle gg| + \text{H.c.}\right\}.$$

$$\text{(B11)}$$

APPENDIX C: THE ENERGETIC COSTS OF THE FEEDBACK CONTROL

Initially, the total energy of the system is $E_S(0) = \text{Tr}[H_S\rho(0)] = \omega_0$, in which $H_S = H_C + H_B$. According to Eq. (B11), in the presence of feedback control ($\omega = 0.5\pi$), the steady state of the system is $\rho_{ss}^1 = |\psi_1\rangle\langle\psi_1|$, in which $|\psi_1\rangle = \sin\theta|e\rangle_C|g\rangle_B - \cos\theta|g\rangle_C|e\rangle_B$, and the corresponding total energy of the system in the steady-state is $E_S^1(\infty) = \omega_0(\cos^2\theta + \sin^2\theta) = \omega_0$, which is equal to the total energy $E_S(0)$ of the initial system. In the absence of feedback control ($\omega = 0$), the steady state of the system is $\rho_{ss}^2 = \sin^2\theta|\psi_1\rangle\langle\psi_1| + \cos^2\theta|gg\rangle\langle gg|$, and the corresponding total energy of the system in the steady-state is $E_S^2(\infty) = \omega_0 \sin^2\theta$, which is less than the total energy $E_S(0)$ of the initial system. It means that a part of the energy is dissipated to the environment.

Through the above analysis, we can see that the feedback suppresses the decay of the system to the double ground state $|gg\rangle\langle gg|$, to keep the total energy of the system unchanged. However, the environmental noise will push the state of the system away from the target state ρ_{ss}^1 constantly, the total energy of the system will be reduced, which means that the controller must provide the same amount of energy to recover this change. Therefore, we define the energy provided by the controller as energy cost, i.e.,

$$\Delta E(\infty) = \text{Tr}[H_S\rho_{ss}^1] - \text{Tr}[H_S\rho_{ss}^2]. \quad \text{(C1)}$$

In Fig. 11, $\Delta E(\infty)$ is displayed as a function of θ, which describes the energy cost for different values of θ. We find that the cost of feedback energy increases as the value of θ decreases.
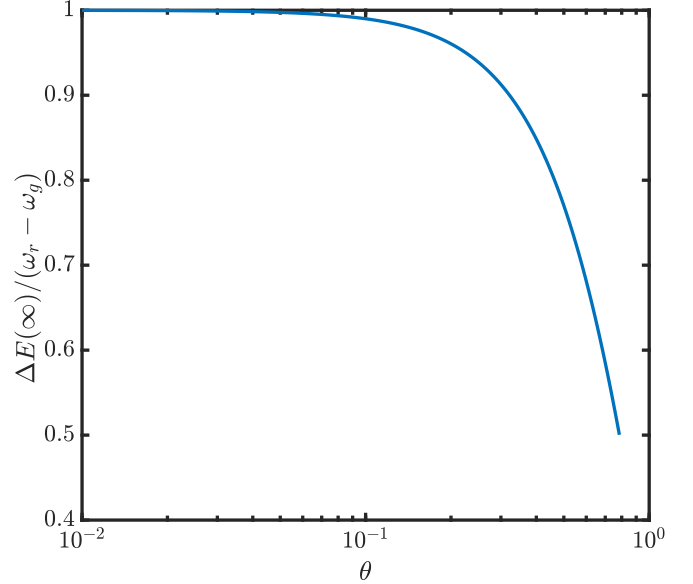

FIG. 11. $\Delta E(\infty)$ as a function of θ, representing the difference in steady state energy between the feedback system and the nonfeedback system. Other parameters are given as $\theta = \pi/12$ and $\omega = 0.5\pi$.

APPENDIX D: FOR DETAILS OF CALCULATING ERGOTROPY

According to Ref. [36], the Hamiltonian H_B and the state ρ_B of the QB that can be expressed by their respective eigenbasis

$$H_B = \sum_n e_n|e_n\rangle\langle e_n|, \quad \text{(D1)}$$

$$\rho_B = \sum_n r_n|r_n\rangle\langle r_n|, \quad \text{(D2)}$$

where $|e_n\rangle$ and $|r_n\rangle$ represent the eigenvectors of H_B and ρ_B, respectively, and $e_0 \leqslant e_1 \leqslant \cdots$ and $r_0 \geqslant r_1 \geqslant \cdots$ are the related eigenvalues, which have been properly ordered. The form of the passive state is

$$\rho^p \equiv \sum_n r_n|e_n\rangle\langle e_n|, \quad \text{(D3)}$$

and its mean energy is $E_p \equiv \text{Tr}[H_B\rho^p] = \sum_n r_n e_n$, which corresponds to the minimum of the Eq. (17), i.e., $E_p = \min_U \text{Tr}[U\rho_B(t)U^\dagger H_B]$. Thus, the ergotropy Σ_B of the state ρ_B can be expressed as

$$\Sigma_B = E_B - E_p = \text{Tr}[H_B(\rho_B - \rho^p)]. \quad \text{(D4)}$$

Consider the case of the QB with a Hamiltonian of the form $H_B = \omega_0\sigma^+\sigma^-$, the density matrix can be expressed as

$$\rho_B = \frac{1}{2}(\mathbb{I} + \vec{r} \cdot \vec{\sigma}), \quad \text{(D5)}$$

where $\mathbb{I}$ is the 2×2 identity, and $\vec{\sigma} \equiv (\sigma^x, \sigma^y, \sigma^z)$ and $\vec{r}$ are the Pauli and Bloch vectors, respectively. According to Eqs. (D3) and (D4), the Σ_B reads

$$\Sigma_B = \frac{\omega_0}{2}(r + r_z), \quad \text{(D6)}$$

where $r = |\vec{r}|$. The ergotropy can be rewritten in term of expectation values of operators as

$$\Sigma_B = \frac{\omega_0}{2}(\sqrt{\langle\sigma_z\rangle^2 + 4\langle\sigma_+\rangle\langle\sigma_-\rangle} + \langle\sigma_z\rangle). \qquad (D7)$$

According to Eqs. (B1) and (D7), the ergotropy of the QB finally reads

$$\Sigma_B(t) = \frac{\omega_0}{2}\{\sqrt{4|\rho_{12}(t) + \rho_{34}(t)|^2 + (2[\rho_{11}(t) + \rho_{33}(t)] - 1)^2}$$
$$+ 2[\rho_{11}(t) + \rho_{33}(t)] - 1\}. \qquad (D8)$$

Accordingly, the energy stored by the QB is

$$\Delta E_B(t) = \omega_0[\rho_{11}(t) + \rho_{33}(t)]. \qquad (D9)$$

APPENDIX E: DERIVATION OF QUANTUM MASTER EQS. (26)~(29)

In the Sec. III, considering the operability of the experiment, we design a Rydberg QB model, in which a dissipative optical cavity is introduced to assist QB charging. Under the Born-Markov approximation, the evolution of the system is governed by the master equation of Eq. (27),

$$\dot{\rho} = -ig_{\text{eff}}[J^+a + J^-a^\dagger, \rho] + \mathcal{L}_\kappa\rho + \mathcal{L}_\gamma\rho. \qquad (E1)$$

For a strongly damped cavity mode, the effect of the highly excited cavity modes is weak, which can be regarded as perturbations. Therefore, we use the photon number to represent the density operator as [62]

$$\dot{\rho} = \sum_{m,n=0}^{1} \rho_{mn}|m\rangle_c\langle n|, \qquad (E2)$$

in which ρ_{mn} is the density matrix elements based on the photon number states of the cavity mode. By substituting Eq. (E2) into the Eq. (E1), the following corresponding coupling equations can be obtained:

$$\dot{\rho}_{00} = \mathcal{L}\rho_{00} - ig_{\text{eff}}[J^+\rho_{10} - \rho_{01}J^-] + \kappa\rho_{11}, \qquad (E3)$$

$$\dot{\rho}_{10} = \mathcal{L}\rho_{10} - ig_{\text{eff}}[J^-\rho_{00} - \rho_{11}J^-] - \tfrac{1}{2}\kappa\rho_{10}, \qquad (E4)$$

$$\dot{\rho}_{01} = \mathcal{L}\rho_{01} - ig_{\text{eff}}[J^+\rho_{11} - \rho_{00}J^+] - \tfrac{1}{2}\kappa\rho_{01}, \qquad (E5)$$

$$\dot{\rho}_{11} = \mathcal{L}\rho_{11} - ig_{\text{eff}}[J^-\rho_{01} - \rho_{10}J^+] - \kappa\rho_{11}, \qquad (E6)$$

where $\mathcal{L}\rho_{ij}$ stands for terms independent of photons. In comparison, ρ_{10} changes more slowly because the most populated state of the cavity mode is the vacuum state. Therefore, it is reasonable to take $\dot{\rho}_{10} = 0$. The following result is obtained:

$$\rho_{10} = \rho_{01}^\dagger \approx -\frac{2ig_{\text{eff}}}{\kappa}[J^-\rho_{00} - \rho_{11}J^-]. \qquad (E7)$$

Then, by substituting Eq. (E7) into Eqs. (E3) and (E6), we have

$$\dot{\rho}_{00} = \mathcal{L}\rho_{00} - \frac{2g_{\text{eff}}^2}{\kappa}[J^+J^-\rho_{00} + \rho_{00}J^+J^- - 2J^+\rho_{11}J^-]$$
$$+ \kappa\rho_{11}, \qquad (E8)$$

$$\dot{\rho}_{11} = \mathcal{L}\rho_{11} - \frac{2g_{\text{eff}}^2}{\kappa}[J^-J^+\rho_{11} + \rho_{11}J^-J^+ - 2J^-\rho_{00}J^+]$$
$$- \kappa\rho_{11}. \qquad (E9)$$

The above two terms characterize the dynamic evolution of atoms. Now we add them together and adiabatically eliminate ρ_{11}, the master equation for the reduced density operator of atoms becomes

$$\dot{\rho} = \Gamma\mathcal{L}[J^-]\rho + \mathcal{L}_\gamma\rho, \qquad (E10)$$

where $\Gamma = 4g_{\text{eff}}^2/\kappa$ is the collective amplitude damping rate of the transition from $|r\rangle$ to $|g\rangle$. If the collective decay rate is much large than the spontaneous emission rate, i.e., $\Gamma \gg \gamma$, then an effective master equation can be expressed as

$$\dot{\rho} = \Gamma\mathcal{L}[J^-]\rho. \qquad (E11)$$

APPENDIX F: THE EFFECT OF THE FINITE TEMPERATURE

If temperature is considered in our scheme, then Eq. (31) in the text should be modified as

$$\rho = -ig_{\text{eff}}[(J^+a + J^-a^\dagger), \rho] + \kappa(n_{\text{th}} + 1)\mathcal{L}[U_{\text{fb}}a]\rho$$
$$+ \kappa n_{\text{th}}\mathcal{L}[a^\dagger]\rho, \qquad (F1)$$

where we have ignored the spontaneous emission of atoms because Rydberg atoms have a low spontaneous emission rate. $n_{\text{th}} = [\exp(\hbar\omega_c/k_BT) - 1]^{-1}$ is the average number of photons, $n_{\text{th}} = 0$ corresponding to $T = 0$.

When considering a zero temperature environment, the Rydberg interaction has no effect on our results, so the feedback operator is expressed as $U_{\text{fb}} = \exp\{-i\omega[(|g\rangle_C\langle r| + |r\rangle_C\langle g|) \otimes I_B]\}$. However, when there is a finite temperature, the system may be excited to the double Rydberg state. Therefore, the Rydberg interaction will be considered, and the corresponding feedback operator is $U_{\text{fb}} = \exp\{-i\lambda[(|g\rangle_C\langle r| + |r\rangle_C\langle g|) \otimes$
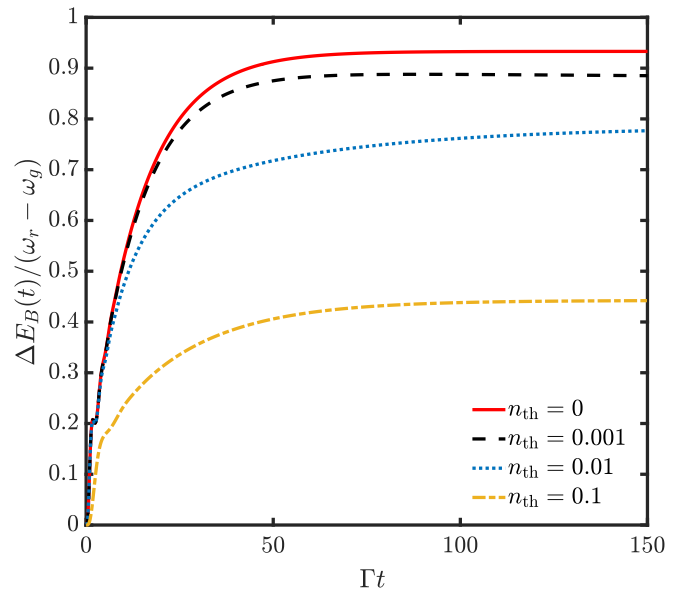

FIG. 12. The stored energy $\Delta E_B(t)$ of the QB as a function of Γt with different n_{th}. The red solid line: $n_{\text{th}} = 0$; The black dashed line: $n_{\text{th}} = 0.001$; The blue dotted line: $n_{\text{th}} = 0.01$; The yellow dash-dotted line: $n_{\text{th}} = 0.1$. The dimension of cavity mode is $N_c = 5$. Other parameters are given as $\kappa = 2.5\Gamma$, $g_{\text{eff}} = 2.5\Gamma$, $U = 500\Gamma$, $\theta = \pi/12$, and $\omega = 0.5\pi$.

$I_B + \frac{U}{\lambda}|rr\rangle\langle rr|]\delta t\}$. Under the strong Rydberg interaction mechanism, this feedback operator can be approximated as $U_{fb} = \exp\{-i\lambda[(|g\rangle_C\langle r| + |r\rangle_C\langle g|) \otimes |g\rangle_B\langle g|]\delta t\}$, where the single-qubit-flip operation of the charger is equivalent to the controlled-flip operation in the strong Rydberg blocked regime. According to the definition $\omega = \lambda\delta t$, the U_{fb} can be rewritten as $U_{fb} = \exp\{-i\omega[(|g\rangle_C\langle r| + |r\rangle_C\langle g|) \otimes |g\rangle_B\langle g|]\}$. In Fig. 12, we plot the stored energy $\Delta E_B(t)$ of the QB as a function of Γt with different n_{th}. Although the stored energy of the QB decreases with the increase of temperature, we can still obtain higher values in the low temperature range ($n_{th} \in [0, 0.01]$), compared with the result in Ref. [53], where the maximum stored energy of QB in the steady state is close to $0.5\omega_0$ in existence of the temperature.

APPENDIX G: DERIVATION OF MASTER EQ. (32)

Due to the limited response time of the device, there is a time delay in the actual feedback control. Therefore, an approximate master equation is derived, which is effective in the limit case of small but not negligible feedback delay. The perturbation method is adopted in the whole process. Combine the details of Secs. II B and IID in Ref. [55], the first-order approximate equation related to the delay time τ is obtained,

$$\dot{\rho}(t) = \{\mathcal{D}_0 + \mathcal{L}[a]\}\rho(t) + (e^{\mathcal{K}} - 1)e^{\mathcal{D}\tau}\mathcal{J}[a]\rho(t - \tau), \tag{G1}$$

where the internal Hamiltonian evolution has been absorbed into the superoperator $\mathcal{D}_0\rho(t)$. $\mathcal{K}$ is a Liouville superoperator, in a special case, $\mathcal{K}\rho = -i[\omega[(|g\rangle_C\langle r| + |r\rangle_C\langle g|) \otimes I_B], \rho]$, $\mathcal{D}\rho \equiv -ig_{eff}[(J^+a + J^-a^\dagger), \rho] + \kappa\mathcal{L}[U_{fb}a]\rho$, and $\mathcal{J}[a]\rho = a\rho a^\dagger$. It must be emphasized that the above equation is only an approximate solution. Then, one can use $e^{\mathcal{D}\tau} \simeq 1 + \mathcal{D}\tau$ and $\rho(t - \tau) \simeq (1 - \mathcal{D}\tau)\rho(t)$ and substitute these terms into Eq. (G1), we obtain

$$\dot{\rho} = [\mathcal{D} + \tau(e^{\mathcal{K}} - 1)\{\mathcal{D}\mathcal{J}[a] - \mathcal{J}[a]\mathcal{D}\}]\rho. \tag{G2}$$

This master equation is equal to the instantaneous feedback master Eq. (31), plus a correction linear in τ.

[1] M. Hiramoto, Y. Kishigami, and M. Yokoyama, Doping effect on the two-layer organic solar cell, Chem. Lett. **19**, 119 (1990).

[2] R. Alicki and M. Fannes, Entanglement boost for extractable work from ensembles of quantum batteries, Phys. Rev. E **87**, 042123 (2013).

[3] E. Schrödinger, Discussion of probability relations between separated systems, Math. Proc. Cambridge Philos. Soc. **31**, 555 (1935).

[4] R. Horodecki, P. Horodecki, M. Horodecki, and K. Horodecki, Quantum entanglement, Rev. Mod. Phys. **81**, 865 (2009).

[5] T. Baumgratz, M. Cramer, and M. B. Plenio, Quantifying Coherence, Phys. Rev. Lett. **113**, 140401 (2014).

[6] S. Luo, Quantum discord for two-qubit systems, Phys. Rev. A **77**, 042303 (2008).

[7] X. X. Li, H. D. Yin, D. X. Li, and X. Q. Shao, Deterministic generation of maximally discordant mixed states by dissipation, Phys. Rev. A **101**, 012329 (2020).

[8] X.-M. Hu, C. Zhang, B.-H. Liu, Yu Cai, X.-J. Ye, Yu Guo, W.-B. Xing, C.-X. Huang, Y.-F. Huang, C.-F. Li, and G.-C. Guo, Experimental High-Dimensional Quantum Teleportation, Phys. Rev. Lett. **125**, 230501 (2020).

[9] E. Olofsson, P. Samuelsson, N. Brunner, and P. P. Potts, Quantum teleportation of single-electron states, Phys. Rev. B **101**, 195403 (2020).

[10] C. Lupo, Subwavelength quantum imaging with noisy detectors, Phys. Rev. A **101**, 022323 (2020).

[11] L. Maccone and C. Ren, Quantum Radar, Phys. Rev. Lett. **124**, 200503 (2020).

[12] S. Jain, J. Alonso, M. Grau, and J. P. Home, Scalable Arrays of Micro-Penning Traps for Quantum Computing and Simulation, Phys. Rev. X **10**, 031027 (2020).

[13] C. Tutschku, R. W. Reinthaler, C. Lei, A. H. MacDonald, and E. M. Hankiewicz, Majorana-based quantum computing in nanowire devices, Phys. Rev. B **102**, 125407 (2020).

[14] E. P. G. Gale, Z. Mehdi, L. M. Oberg, A. K. Ratcliffe, S. A. Haine, and J. J. Hope, Optimized fast gates for quantum computing with trapped ions, Phys. Rev. A **101**, 052328 (2020).

[15] F. Campaioli, F. A. Pollock, F. C. Binder, L. Céleri, J. Goold, S. Vinjanampathy, and K. Modi, Enhancing the Charging Power of Quantum Batteries, Phys. Rev. Lett. **118**, 150601 (2017).

[16] G. M. Andolina, M. Keck, A. Mari, M. Campisi, V. Giovannetti, and M. Polini, Extractable Work, the Role of Correlations, and Asymptotic Freedom in Quantum Batteries, Phys. Rev. Lett. **122**, 047702 (2019).

[17] T. P. Le, J. Levinsen, K. Modi, M. M. Parish, and F. A. Pollock, Spin-chain model of a many-body quantum battery, Phys. Rev. A **97**, 022106 (2018).

[18] Yu-Yu Zhang, T.-R. Yang, L. Fu, and X. Wang, Powerful harmonic charging in a quantum battery, Phys. Rev. E **99**, 052106 (2019).

[19] D. Ferraro, M. Campisi, G. M. Andolina, V. Pellegrini, and M. Polini, High-Power Collective Charging of a Solid-State Quantum Battery, Phys. Rev. Lett. **120**, 117702 (2018).

[20] G. M. Andolina, D. Farina, A. Mari, V. Pellegrini, V. Giovannetti, and M. Polini, Charger-mediated energy transfer in exactly solvable models for quantum batteries, Phys. Rev. B **98**, 205423 (2018).

[21] A. Crescente, M. Carrega, M. Sassetti, and D. Ferraro, Ultrafast charging in a two-photon Dicke quantum battery, Phys. Rev. B **102**, 245407 (2020).

[22] F. H. Kamin, F. T. Tabesh, S. Salimi, and A. C. Santos, Entanglement, coherence, and charging process of quantum batteries, Phys. Rev. E **102**, 052109 (2020).

[23] L. Peng, W.-B. He, S. Chesi, H.-Q. Lin, and X.-W. Guan, Lower and upper bounds of quantum battery power in multiple central spin systems, Phys. Rev. A **103**, 052220 (2021).

[24] G. M. Andolina, M. Keck, A. Mari, V. Giovannetti, and M. Polini, Quantum versus classical many-body batteries, Phys. Rev. B **99**, 205437 (2019).

[25] F. Caravelli, G. Coulter-De Wit, L. P. García-Pintos, and A. Hamma, Random quantum batteries, Phys. Rev. Res. **2**, 023095 (2020).

[26] S. Julià-Farré, T. Salamon, A. Riera, M. N. Bera, and M. Lewenstein, Bounds on the capacity and power of quantum batteries, Phys. Rev. Res. **2**, 023113 (2020).

[27] D. Rossini, G. M. Andolina, and M. Polini, Many-body localized quantum batteries, Phys. Rev. B **100**, 115142 (2019).

[28] M. Alimuddin, T. Guha, and P. Parashar, Structure of passive states and its implication in charging quantum batteries, Phys. Rev. E **102**, 022106 (2020).

[29] F. C. Binder, S. Vinjanampathy, K. Modi, and J. Goold, Quantacell: Powerful charging of quantum batteries, New J. Phys. **17**, 075015 (2015).

[30] A. Crescente, M. Carrega, M. Sassetti, and D. Ferraro, Charging and energy fluctuations of a driven quantum battery, New J. Phys. **22**, 063057 (2020).

[31] A. C. Santos, A. Saguia, and M. S. Sarandy, Stable and charge-switchable quantum batteries, Phys. Rev. E **101**, 062114 (2020).

[32] L. F. C. Moraes, A. Saguia, A. C. Santos, and M. S. Sarandy, Charging power and stability of always-on transitionless driven quantum batteries, Europhys. Lett. (2021), doi:10.1209/0295-5075/ac1363.

[33] A. C. Santos, B. Çakmak, S. Campbell, and N. T. Zinner, Stable adiabatic quantum batteries, Phys. Rev. E **100**, 032107 (2019).

[34] F.-Q. Dou, Y.-J. Wang, and J.-A. Sun, Closed-loop three-level charged quantum battery, Europhys. Lett. **131**, 43001 (2020).

[35] F. Barra, Dissipative Charging of a Quantum Battery, Phys. Rev. Lett. **122**, 210601 (2019).

[36] D. Farina, G. M. Andolina, A. Mari, M. Polini, and V. Giovannetti, Charger-mediated energy transfer for quantum batteries: An open-system approach, Phys. Rev. B **99**, 035421 (2019).

[37] K. Ito and G. Watanabe, Collectively enhanced high-power and high-capacity charging of quantum batteries via quantum heat engines, arXiv:2008.07089.

[38] F. T. Tabesh, F. H. Kamin, and S. Salimi, Environment-mediated charging process of quantum batteries, Phys. Rev. A **102**, 052223 (2020).

[39] J. Q. Quach, K. E. McGhee, L. Ganzer, D. M. Rouse, B. W. Lovett, E. M. Gauger, J. Keeling, G. Cerullo, D. G. Lidzey, and T. Virgili, An organic quantum battery, arXiv:2012.06026.

[40] F. Pirmoradian and K. Mølmer, Aging of a quantum battery, Phys. Rev. A **100**, 043833 (2019).

[41] F. Tacchino, T. F. F. Santos, D. Gerace, M. Campisi, and M. F. Santos, Charging a quantum battery via nonequilibrium heat current, Phys. Rev. E **102**, 062133 (2020).

[42] S. Gherardini, F. Campaioli, F. Caruso, and F. C. Binder, Stabilizing open quantum batteries by sequential measurements, Phys. Rev. Res. **2**, 013095 (2020).

[43] T.-R. Yang, Yu-Yu Zhang, H. Dong, L. Fu, and X. Wang, Optimal building block of multipartite quantum battery, arXiv:2010.09970.

[44] F. Zhao, F.-Q. Dou, and Q. Zhao, Quantum battery of interacting spins with environmental noise, Phys. Rev. A **103**, 033715 (2021).

[45] L. P. García-Pintos, A. Hamma, and A. del Campo, Fluctuations in Extractable Work Bound the Charging Power of Quantum Batteries, Phys. Rev. Lett. **125**, 040601 (2020).

[46] S. Ghosh, T. Chanda, S. Mal, and A. Sen(De), Fast charging of quantum battery assisted by noise, Phys. Rev. A **104**, 032207 (2021).

[47] X. Zhang and M. blaauboer, Enhanced energy transfer in a dicke quantum battery, arXiv:1812.10139.

[48] S.-Y. Bai and J.-H. An, Floquet engineering to reactivate a dissipative quantum battery, Phys. Rev. A **102**, 060201(R) (2020).

[49] S. Ghosh, T. Chanda, and A. Sen(De), Enhancement in the performance of a quantum battery by ordered and disordered interactions, Phys. Rev. A **101**, 032115 (2020).

[50] M. Carrega, A. Crescente, D. Ferraro, and M. Sassetti, Dissipative dynamics of an open quantum battery, New J. Phys. **22**, 083085 (2020).

[51] C. L. Latune, I. Sinayskiy, and F. Petruccione, Energetic and entropic effects of bath-induced coherences, Phys. Rev. A **99**, 052105 (2019).

[52] K. V. Hovhannisyan, F. Barra, and A. Imparato, Charging assisted by thermalization, Phys. Rev. Res. **2**, 033413 (2020).

[53] J. Q. Quach and W. J. Munro, Using Dark States to Charge and Stabilize Open Quantum Batteries, Phys. Rev. Appl. **14**, 024092 (2020).

[54] M. T. Mitchison, J. Goold, and J. Prior, Charging a quantum battery with linear feedback control, Quantum **5**, 500 (2021).

[55] H. M. Wiseman, Quantum theory of continuous feedback, Phys. Rev. A **49**, 2133 (1994).

[56] P. Barberis-Blostein, D. G. Norris, L. A. Orozco, and H. J. Carmichael, From quantum feedback to probabilistic error correction: Manipulation of quantum beats in cavity qed, New J. Phys. **12**, 023002 (2010).

[57] C. Ahn, A. C. Doherty, and A. J. Landahl, Continuous quantum error correction via quantum feedback control, Phys. Rev. A **65**, 042301 (2002).

[58] S. S. Szigeti, A. R. R. Carvalho, J. G. Morley, and M. R. Hush, Ignorance is Bliss: General and Robust Cancellation of Decoherence Via No-Knowledge Quantum Feedback, Phys. Rev. Lett. **113**, 020407 (2014).

[59] D. Vitali, S. Zippilli, P. Tombesi, and J.-M. Raimond, Decoherence control with fully quantum feedback schemes, J. Mod. Opt. **51**, 799 (2004).

[60] M. Schemmer, A. Johnson, R. Photopoulos, and I. Bouchoule, Monte Carlo wave-function description of losses in a one-dimensional Bose gas and cooling to the ground state by quantum feedback, Phys. Rev. A **95**, 043641 (2017).

[61] P. Rabl, V. Steixner, and P. Zoller, Quantum-limited velocity readout and quantum feedback cooling of a trapped ion via electromagnetically induced transparency, Phys. Rev. A **72**, 043823 (2005).

[62] J. Wang, H. M. Wiseman, and G. J. Milburn, Dynamical creation of entanglement by homodyne-mediated feedback, Phys. Rev. A **71**, 042309 (2005).

[63] X.-Q. Shao, T.-Y. Zheng, and S. Zhang, Engineering steady three-atom singlet states via quantum-jump-based feedback, Phys. Rev. A **85**, 042308 (2012).

[64] X. Q. Shao, Z. H. Wang, H. D. Liu, and X. X. Yi, Dissipative preparation of a tripartite singlet state in coupled arrays of cavities via quantum feedback control, Phys. Rev. A **94**, 032307 (2016).

[65] I. M. Mirza and J. C. Schotland, Multiqubit entanglement in bidirectional-chiral-waveguide qed, Phys. Rev. A **94**, 012302 (2016).

[66] A. E Allahverdyan, R. Balian, and T. M. Nieuwenhuizen, Maximal work extraction from finite quantum systems, Europhys. Lett. **67**, 565 (2004).

[67] G. Francica, J. Goold, F. Plastina, and M. Paternostro, Daemonic ergotropy: Enhanced work extraction from quantum correlations, npj Quantum Inf. **3**, 12 (2017).

[68] W. Pusz and S. L. Woronowicz, Passive states and KMS states for general quantum systems, Commun. Math. Phys. **58**, 273 (1978).

[69] M. Perarnau-Llobet, K. V. Hovhannisyan, M. Huber, P. Skrzypczyk, J. Tura, and A. Acín, Most energetic passive states, Phys. Rev. E **92**, 042147 (2015).

[70] Y. O. Dudin, L. Li, F. Bariani, and A. Kuzmich, Observation of coherent many-body Rabi oscillations, Nat. Phys. **8**, 790 (2012).

[71] X. L. Zhang, L. Isenhower, A. T. Gill, T. G. Walker, and M. Saffman, Deterministic entanglement of two neutral atoms via Rydberg blockade, Phys. Rev. A **82**, 030306(R) (2010).

[72] X. L. Zhang, A. T. Gill, L. Isenhower, T. G. Walker, and M. Saffman, Fidelity of a Rydberg-blockade quantum gate from simulated quantum process tomography, Phys. Rev. A **85**, 042310 (2012).

[73] T. A. Johnson, E. Urban, T. Henage, L. Isenhower, D. D. Yavuz, T. G. Walker, and M. Saffman, Rabi Oscillations Between Ground and Rydberg States with Dipole-Dipole Atomic Interactions, Phys. Rev. Lett. **100**, 113003 (2008).

[74] A. Öttl, S. Ritter, M. Köhl, and T. Esslinger, Hybrid apparatus for Bose-Einstein condensation and cavity quantum electrodynamics: Single atom detection in quantum degenerate gases, Rev. Sci. Instrum. **77**, 063118 (2006).

[75] F. Brennecke, T. Donner, S. Ritter, T. Bourdel, M. Köhl, and T. Esslinger, Cavity QED with a Bose-Einstein condensate, Nature (London) **450**, 268 (2007).

[76] C. Guerlin, E. Brion, T. Esslinger, and K. Mølmer, Cavity quantum electrodynamics with a Rydberg-blocked atomic ensemble, Phys. Rev. A **82**, 053832 (2010).

[77] X.-F. Zhang, Q. Sun, Y.-C. Wen, W.-M. Liu, S. Eggert, and A.-C. Ji, Rydberg Polaritons in a Cavity: A Superradiant Solid, Phys. Rev. Lett. **110**, 090402 (2013).

[78] A. Grankin, E. Brion, E. Bimbard, R. Boddeda, I. Usmani, A. Ourjoumtsev, and P. Grangier, Quantum statistics of light transmitted through an intracavity Rydberg medium, New J. Phys. **16**, 043020 (2014).